The influence of clouds and diffuse radiation on ecosystem-atmosphere CO_2 and $CO^{18}O$ exchanges

[1,2]Still, C.J., [3]Riley, W.J., [3]Biraud, S.C., [4]Noone, D.C., [4]Buenning, N.H., [5]Randerson J.T., [3]Torn, M.S., [6]Welker, J., [7]White, J.W.C., [7]Vachon, R., [8]Farquhar, G.D., and [9]Berry, J.A.

1. Geography Department, University of California, Santa Barbara, CA USA
2. Institute for Computational Earth System Science, University of California, Santa Barbara, CA USA
3. Earth Sciences Division, Lawrence Berkeley National Laboratory, Berkeley, CA USA
4. Department of Atmospheric and Oceanic Sciences, and Cooperative Institute for Research in Environmental Science, University of Colorado, Boulder, CO USA
5. Earth System Science Department, University of California, Irvine, CA USA
6. Environment and Natural Resources Institute, University of Alaska, Anchorage, AK USA
7. INSTAAR, and Cooperative Institute for Research in Environmental Science, University of Colorado, Boulder, CO USA
8. Research School of Biological Sciences, Australian National University, Canberra, ACT Australia
9. Department of Global Ecology, Carnegie Institution of Washington, Stanford, CA USA

Index terms: 0426, 0321, 0414, 0454, 0428

Keywords: clouds, oxygen isotope discrimination, diffuse radiation, photosynthesis, isofluxes

Abstract

This study evaluates the potential impact of clouds on ecosystem CO_2 and CO_2 isotope fluxes ('isofluxes') in two contrasting ecosystems (a broadleaf deciduous forest and a C_4 grassland), in a region for which cloud cover, meteorological, and isotope data are available for driving the isotope-enabled land surface model, ISOLSM. Our model results indicate a large impact of clouds on ecosystem CO_2 fluxes and isofluxes. Despite lower irradiance on partly cloudy and cloudy days, predicted forest canopy photosynthesis was substantially higher than on clear, sunny days, and the highest carbon uptake was achieved on the cloudiest day. This effect was driven by a large increase in light-limited shade leaf photosynthesis following an increase in the diffuse fraction of irradiance. Photosynthetic isofluxes, by contrast, were largest on partly cloudy days, as leaf water isotopic composition was only slightly depleted and photosynthesis was enhanced, as compared to adjacent clear sky days. On the cloudiest day, the forest exhibited intermediate isofluxes: although photosynthesis was highest on this day, leaf-to-atmosphere isofluxes were reduced from a feedback of transpiration on canopy relative humidity and leaf water. Photosynthesis and isofluxes were both reduced in the C_4 grass canopy with increasing cloud cover and diffuse fraction as a result of near-constant light limitation of photosynthesis. These results suggest that some of the unexplained variation in global mean $\delta^{18}O$ of CO_2 may be driven by large-scale changes in clouds and aerosols and their impacts on diffuse radiation, photosynthesis, and relative humidity.

1. Introduction

While spatial and temporal variations in atmospheric CO_2 and its $^{13}C/^{12}C$ composition have received considerable attention from the carbon cycle community (e.g., Ciais *et al.* 1995; Fung *et al.* 1997; Rayner *et al.* 1999, 2008; Randerson *et al.* 2002a,b; Scholze *et al.* 2003), much less is known about the $^{18}O/^{16}O$ composition of atmospheric CO_2 ($\delta^{18}O_a$ - symbols defined in Table 1). Although global simulations of $\delta^{18}O_a$ and its controlling processes have made good progress (Farquhar *et al.* 1993; Ciais *et al.* 1997a,b; Peylin *et al.* 1999; Cuntz *et al.* 2003a,b; Buenning *et al., in prep*), fundamental spatial and temporal variations of $\delta^{18}O_a$ are poorly captured by state-of-the-art global model simulations. One example of unexplained behavior is the phase shift between seasonal cycles of CO_2 and $\delta^{18}O_a$ observed at high northern latitudes, though a recent study showed how this shift is sensitive to boreal forest plant functional type composition and the $\delta^{18}O$ of plant source water (Welp *et al.* 2006). A second, outstanding example of unexplained variation is the large, multi-year variation in mean $\delta^{18}O_a$ observed at many stations. The pronounced downward excursion in global mean $\delta^{18}O_a$ observed during the early and mid-1990s averaged ~ -0.1‰ yr^{-1} for extratropical, marine boundary layer stations, implying isotope fluxes, or 'isofluxes,' on the order of tens of Pmol CO_2 ‰ yr^{-1}.

Because $\delta^{18}O_a$ is strongly influenced by exchanges of $CO^{18}O$ between the atmosphere and terrestrial ecosystems during photosynthesis and respiration (Francey and Tans 1987; Friedli *et al.* 1987; Farquhar *et al.* 1993; Ciais *et al.* 1997a,b; Cuntz *et al.* 2003a,b), several studies have related the downward excursion of $\delta^{18}O_a$ to terrestrial carbon cycle anomalies (Gillon and Yakir 2001; Stern *et al.* 2001; Ishizawa *et al.* 2002; Flanagan 2005). However, water cycle anomalies can also affect $\delta^{18}O_a$, as the $\delta^{18}O$ of ecosystem-to-atmosphere CO_2 fluxes is determined by the $\delta^{18}O$ of leaf and soil water pools which interact with CO_2 during photosynthesis and respiration (Yakir and Sternberg 2000). Leaf and soil water $\delta^{18}O$ are in turn determined by the $\delta^{18}O$ of precipitation (Welker 2000, Vachon *et al.* 2007) and water vapor and subsequent isotopic fractionations during evaporation and diffusion (Craig and Gordon 1965; Allison *et al.* 1983). Although either carbon or water cycle anomalies may drive $\delta^{18}O_a$, unexplained multi-year variations in $\delta^{18}O_a$ such as occurred in the 1990s likely result from linked perturbations to both cycles.

Recent research has documented large variability in tropical cloud cover (e.g., Wielicki *et al.* 2002) on interannual timescales that span part of the $\delta^{18}O_a$ record. For example, satellite measurements of earth's shortwave and longwave radiation budgets over the 1990s suggest decreases in tropical mean cloudiness (Wielicki *et al.* 2002), in agreement with decreases in the monthly mean global cloud fraction over the 1990s (http://isccp.giss.nasa.gov/climanal1.html). Tropical cloud cover variability may be particularly relevant for understanding global $\delta^{18}O_a$ variations, as tropical terrestrial ecosystem CO_2 fluxes comprise a large fraction global productivity. Other satellite-based analyses document increasing spring and summer cloud cover in the Arctic region (Wang and Key 2003). In addition, evidence from ground-based radiometers suggests secular changes in surface global irradiance, with a total reduction of ~4-6% from about 1960 to 1990 ('global dimming'- Stanhill and Cohen 2001; Liepert 2002; Liepert *et al.* 2004) followed by a reversal from roughly 1990 onwards that has been termed 'global brightening' (Wild *et al*. 2005, 2007; Pinker *et al.* 2005; Roderick 2006).

Here we examine the hypothesis that these large-scale changes in cloud cover and irradiance account for part of the unexplained variation observed in $\delta^{18}O_a$, as clouds influence several environmental factors important in controlling biosphere-atmosphere CO_2 isofluxes. Clouds reduce total shortwave (global) irradiance (R_S) while also increasing diffuse irradiance (R_D) and the diffuse fraction (R_D/R_S, the ratio of diffuse irradiance to total or global irradiance - Roderick 1999). Numerous empirical and theoretical studies have noted the impact of changes in diffuse photosynthetically active radiation (PAR) on canopy carbon uptake via increases in photosynthesis of light-limited shade leaves and other associated changes in the environment (e.g., Price and Black 1990; Hollinger *et al*. 1994, 1998; Gower *et al*. 1999; Choudhury 2001; Roderick *et al*. 2001; Freedman *et al*. 2001; Gu *et al*. 1999, 2002, 2003; Rocha *et al*. 2004; Min 2005; Urban *et al*. 2007; Oliveira *et al*. 2007; Knohl and Baldocchi 2008). In addition to increasing R_D/R_S and the contribution of shade leaves to canopy photosynthesis, clouds decrease radiant heating of upper canopy sun leaves, potentially increasing photosynthetic rates (Roderick *et al.* 2001; Gu *et al*. 2002, 2003). Increased cloudiness is often also associated with higher surface relative humidity via decreases in air and leaf temperature and increases in specific humidity (Freedman *et al.* 2001).

Relative humidity will influence both photosynthetic CO_2 fluxes and the $\delta^{18}O$ of leaf and soil water via impacts on stomatal conductance, and thus can have a disproportionate impact on ecosystem-atmosphere isofluxes. An increase in relative humidity generally increases stomatal conductance, which, coupled with increased shade leaf photosynthesis, should increase photosynthetic isofluxes. However, increased relative humidity will also decrease leaf water $\delta^{18}O$ due to a greater influx of depleted vapor, and this would decrease photosynthetic isofluxes.

Thus, the *net* effect of changing cloud cover on biosphere-atmosphere CO_2 and CO_2 isofluxes exchanges is difficult to assess without high-frequency ecosystem $CO^{18}O$ flux measurements. However, these data are currently being collected at only a few sites at present (Griffis *et al.* 2008; McDowell *et al.* 2008). The focus of this study instead is to examine potential ecosystem isoflux responses using observed cloud cover, radiation, meteorological and water isotope data to drive an isotope-enabled ecosystem model (ISOLSM). We chose to focus on two contrasting ecosystems in the Southern Great Plains over a short time period for intensive investigation of the mechanisms underlying the modeled canopy isoflux response to changing cloud cover. For our analyses, we selected a 12-day period from July 11-22, 2004 (day of year (DOY) 193-204,) during which strong variations in daytime thick cloud cover occurred at our study site, from less than 10% on clear days to 100% on a cloudy day. In addition to cloud cover variations, we selected this period using the following criteria: constant LAI, only trace amounts of precipitation (since precipitation $\delta^{18}O$ is a primary driver of CO_2 isofluxes), and no large changes in air temperature and specific humidity due to the passage of differing air masses associated with storm fronts. By limiting variability from these factors, we decomposed the predicted isoflux response to cloud cover into its component processes.

2. Methods

2.1 Site Description

To capture the relevant processes that determine the net impact of clouds on ecosystem $CO^{18}O$ isofluxes, we employed a comprehensive, isotope-enabled ecosystem model (ISOLSM – Riley *et al*. 2002, 2003; Still *et al*. 2005) in the DOE Atmospheric Radiation Measurement (ARM) program's Climate Research Facility (ACRF) in the

140,000 km^2 Southern Great Plains (SGP) region of Oklahoma and Kansas (Ackerman and Stokes 2003). The SGP region is particularly amenable for such a study because of the great diversity of cloud property, aerosol, radiation, and meteorological measurements available, with the most intensive data collection at the Central Facility (CF) site near Lamont, OK (36° 36.30' N, 97° 29.10' W, 320 masl). Analysis of atmospheric data collected at the CF has shown large changes in irradiance driven by cloud cover from 1997-2004 (Dong *et al.* 2006). The SGP region also contains natural and agricultural ecosystems representing a variety of photosynthetic pathways and growth forms, including tallgrass prairies, broadleaf forests along riparian areas, and crops such as winter wheat, milo, and corn. Because we wanted to explore the impact of cloud cover variations on ecosystem-atmosphere isofluxes in two globally important but strongly contrasting natural vegetation types also represented within the SGP region, we chose broadleaf deciduous forests and C_4 grasslands for our model simulations.

2.2 Model Description

ISOLSM is based on the NCAR Land Surface Model (LSM1.0 - Bonan 1994; Bonan et al. 1997), which was modified by Riley et al. (2002) to simulate the carbon and oxygen isotope composition of terrestrial ecosystem-atmosphere CO_2 and H_2O exchanges. The model simulates canopy radiation transfer using the two-stream approximation of Dickinson (1983) and Sellers (1985) to calculate direct and diffuse radiation fluxes in the visible and near-infrared wavebands. The canopy is divided into sunlit and shaded leaves using an extinction coefficient that accounts for scattering within the canopy (Sellers 1985). The model does not vary leaf nitrogen and photosynthetic capacity between sun and shade leaves, as is done in some models (e.g., de Pury and Farquhar 1997; Wang and Leuning 1998). The version of ISOLSM applied here differs from that described in Riley *et al.* (2002) by several changes made to the plant photosynthesis submodels. First, low and high temperature inhibition factors on the maximum catalytic capacity of Rubisco (V_{max}) from Sellers *et al.* (1996) have been included. Second, we implemented the method of Sellers *et al.* (1996) to smooth transitions between the three limiting assimilation rates (i.e., Rubisco, light, and export limited). Finally, iterations to estimate C_c and C_i, the leaf chloroplast and internal CO_2 concentrations, are now performed using net photosynthesis (i.e., accounting for leaf respiration occurring inside the leaf), as opposed to gross photosynthesis, as done in the original version of LSM1. Of these changes, the last had the largest impact, resulting in values for V_{max} and C_i that are much closer to measured values. Accurate C_i and C_c are critical for simulating isotopic fractionations against $^{13}CO_2$ and $CO^{18}O$. ISOLSM models mesophyll (or internal) conductance in C_3 plants to be proportional to the maximum carboxylation capacity (V_{max} - μmol m^{-2} s^{-1}) following Evans and Loreto (2000), but without the soil moisture dependence implemented by Randerson *et al*. (2002b). During light-saturated photosynthesis in forest sun leaves, the average drawdown from C_i to C_c was ~4 Pa over the study period, similar to the drawdown measured by Gillon and Yakir (2000).

We have tested ISOLSM's H_2O and CO_2 flux predictions against several sets of measurements: (1) in the dominant vegetation types using measurements (Suyker and Verma, 2001) performed in the SGP as part of the Ameriflux program (Riley *et al.* 2003); (2) against three years of surface measurements made during the FIFE campaign (Betts and Ball 1998; Cooley *et al.* 2005); (3) in a tallgrass prairie site in Kansas (Lai *et al*. 2005); (4) in an old growth conifer forest in Oregon (Aranibar *et al.* 2006); and in more recent measurements in wheat, pasture, and soy (Riley *et al.* to be submitted). We have also tested ISOLSM's isotopic predictions against available data in Great Plains grassland and cropland ecosystems (i.e., $\delta^{18}O$ in ecosystem water pools and fluxes, and $\delta^{18}O$ in ecosystem CO_2 fluxes – Riley *et al.* 2003; Still *et al.* 2005; Lai *et al.* 2005). We have previously applied ISOLSM to examine (1) impacts of the atmospheric $\delta^{18}O$ value of H_2O and CO_2 on ecosystem discrimination against $CO^{18}O$ (Riley *et al*. 2003); (2) impact of carbonic anhydrase activity in soils and leaves (Riley *et al*. 2002, 2003); (3) impacts of gradients in the $\delta^{18}O$ value of near-surface soil water on the $\delta^{18}O$ value of the soil-surface CO_2 flux (Riley *et al*. 2003; Riley 2005); (4) impacts of land-use change on regional surface CO_2 and energy fluxes and near-surface climate (Cooley *et al.* 2005); and (5) the use of ^{13}C measurements to improve model parameterizations (Aranibar *et al.* 2006). The isotope sub-models in ISOLSM simulate the dominant processes impacting the $\delta^{18}O$ value of soil ($\delta^{18}O_{sw}$) and leaf H_2O ($\delta^{18}O_{lw}$) and CO_2 fluxes: advection of $H_2^{18}O$ in soil water and subsequent evaporation, leaf water isotopic enrichment, isotopic exchanges between H_2O and CO_2 in the soil and leaves, the transport of CO_2 and $CO^{18}O$ in the soil column, and the $\delta^{18}O$ of canopy water vapor ($\delta^{18}O_{cv}$). The xylem source water that supplies leaves, $\delta^{18}O_{xy}$, is determined in ISOLSM by the vertical distribution of $\delta^{18}O_{sw}$, weighted by rooting density profiles for the various ecosystem types. $\delta^{18}O_{cv}$ is calculated at each time step as a function of vapor isotope exchanges with above-canopy air ($\delta^{18}O_v$), as well as isotope fluxes from canopy transpiration and soil and canopy evaporation when the canopy is wet (Riley *et al.* 2002). Further description of our leaf water $\delta^{18}O$ and photosynthetic isoflux calculations is given in section 3.

2.3 Cloud Cover, Radiation, Meteorology, and Water Isotope Forcing Data

ISOLSM is forced with meteorological and water isotope data (Riley *et al.* 2002, 2003), and it has recently been modified to ingest satellite measurements of vegetation characteristics such as the projected leaf area index (LAI). For the simulations reported here, radiation, cloud property, and aerosol data were acquired from instruments at the ARM Central Facility (CF) in Lamont, OK, which is the primary measurement facility within the ARM SGP region (Ackerman and Stokes 2003). The instrument array at the CF includes sensors to measure cloud presence and cloud radiative properties, which are necessary to explore the role of clouds in ecosystem-atmosphere $CO^{18}O$ exchanges. Radiation fluxes measured at the CF site include downwelling shortwave radiation (direct and diffuse) and downwelling longwave radiation. For our analysis, early morning and late afternoon values (solar angles less than 15°) were screened to minimize the impact of low solar angles on R_D/R_S.

The ARM cloud data used are the daytime percent cover of clouds, as measured by the total sky imager (TSI), an instrument that measures the fractional sky coverage of thin and thick (opaque) clouds (i.e., the fraction of the hemispheric field-of-view that contains these cloud types) for daytime periods when the solar elevation exceeds 10 degrees. For this analysis, we focus on the percent cover of thick clouds, as these are both the dominant cloud types and have the largest impact on irradiance, R_D/R_S, temperature, and relative humidity. Min (2005) showed that diffuse radiation fluxes due to optically thick clouds have a greater impact on canopy photosynthetic efficiency than do fluxes from optically thin clouds. Because of temporal limitations on these data (i.e., only daytime cloud cover fractions are available from the TSI), we have restricted our analysis to daytime periods. Although nighttime clouds can affect the surface energy budget and carbon cycle through modulation of longwave energy fluxes (e.g., Dai *et al.* 1999), the largest impacts of clouds on canopy isofluxes should occur during the day. Unfortunately, cloud-screened aerosol optical depth data from a sun photometer (e.g., Niyogi et al. 2004; Oliveira *et al*. 2007) were not available for our study period to allow a separate assessment of aerosol impacts on isofluxes.

The meteorological data used to force ISOLSM include air temperature, pressure, water vapor content, wind speed, and precipitation amount. These data were taken from the Oklahoma and Kansas Mesonet program. The Mesonet consists of 145 instrument platforms (as of April 2007) distributed throughout the two states. Each station measures relative humidity, wind speed and direction, air temperature, and atmospheric pressure, and reports these data as 5-minute, 15-minute, or half-hourly averages for the state of Oklahoma and as hourly average for the state of Kansas. Additional external datasets required by ISOLSM included the following: (1) soil type from the 1 km USGS Statsgo soils database (i.e., 20% sand, 15% silt, and 65% clay around the CF); (2) monthly mean precipitation $\delta^{18}O$ values averaged over 2-5 years of data from analyses of archived water samples collected by the EPA National Atmospheric Deposition Program (NADP) network (Lynch *et al*. 1995) between 1980 and 1990 and interpolated across the Great Plains region (Welker 2000); and (3) the atmospheric CO_2 concentration.

The model simulations also require the $\delta^{18}O$ composition of above-canopy water vapor ($\delta^{18}O_v$) and background atmospheric CO_2 ($\delta^{18}O_a$). Neither quantity is measured continuously in this region. Many factors affect $\delta^{18}O_v$ (Lee *et al*. 2006), including evapotranspiration and horizontal and vertical atmospheric advection, and diurnal variations of up to 4‰ have been measured in this area (Helliker *et al*. 2002; Riley *et al*. 2003); smaller diurnal variations (1-2‰) have been observed over temperate forests (Lai *et al*. 2005; Lee *et al*. 2006). Other investigators have shown strong linear or log-linear relationships between specific humidity and $\delta^{18}O_v$ (White and Gedzelman 1984; Lee *et al*. 2006). However, we have no information on this relationship in the SGP region, as extensive $\delta^{18}O_v$ data are not available. Instead, for this set of simulations, we set $\delta^{18}O_v$ to be in a temperature-dependent isotopic equilibrium with the most recent precipitation event (e.g., Lee *et al*. 2006). Although our approach only crudely captures the processes that regulate $\delta^{18}O_v$, the sensitivity of ecosystem-atmosphere $CO^{18}O$ exchanges to diurnal variations in $\delta^{18}O_v$ has been examined in detail by Riley *et al*. (2003) and found to be small, partly because the more important vapor $\delta^{18}O$ is that of within-canopy vapor, $\delta^{18}O_{cv}$, which interacts directly with $\delta^{18}O_{lw}$. Riley *et al.* (2003) also showed that diurnal variations in $\delta^{18}O_a$ can impact CO_2 isofluxes. However, since we lacked consistent diurnal measurements of $\delta^{18}O_a$, we imposed a constant value of -0.5‰, which is similar to the zonal annual mean value from mid-latitude, northern hemisphere stations in the NOAA air sampling network (Cuntz *et al.* 2003b), and is close to mean values measured 3-4 km above the surface by ARM and NOAA. There is no diagnostic solution for the canopy air space CO_2 and $CO^{18}O$ concentrations that is analogous to the H_2O and $H_2{}^{18}O$ solution (Riley *et al.* 2002). We therefore assume that canopy CO_2 and $CO^{18}O$ concentrations are the same as above-canopy values. To properly analyze potential feedbacks between leaf and canopy $CO^{18}O$ fluxes, a prognostic canopy airspace model would need to be used; to our knowledge, no previous work has addressed this issue.

2.4 Model Sensitivity Experiments

Our primary objective was to better understand the effects of cloud cover and associated environmental factors such as diffuse radiation and relative humidity on ecosystem-atmosphere $CO^{18}O$ exchanges for two globally important and strongly contrasting biomes that should bracket the expected range of ecosystem responses to cloud cover: broadleaf deciduous forests and C_4 grasslands. The two types differ in photosynthetic pathway (C_3 forest and C_4 grass), life form (tree versus grass), and canopy stature (canopy heights used in ISOLSM are 20 m and 0.5 m, respectively – Bonan 1996), thereby allowing us to explore a wide range of potential ecosystem CO_2 isoflux responses to cloud cover variations. The LAI values we used are particularly important because a higher diffuse radiation fraction is more influential with higher canopy LAI, as more leaf area is in shade during sunny conditions dominated by direct beam radiation (cf., Roderick *et al*. 2001; Gu *et al*. 2002; Alton *et al*. 2005; Knohl and Baldocchi 2008). To assess the sensitivity of our results to LAI in the broadleaf forest, we ran our base simulation with the mean value (5.0) for temperate broadleaf forests from Asner *et al*. (2003). We also ran simulations with LAI values one standard deviation above and below the mean (i.e., LAI of 3.5 and 6.5, with all other driving variables were held constant). An LAI of 6.5 is not uncommon in temperate and tropical broadleaf forests, which together contribute substantially to global primary production (e.g., Field *et al.* 1998) and thus are particularly relevant for understanding global $\delta^{18}O_a$ variations. We set the C_4 grass canopy LAI to 3.75. This value is typical of highly productive C_4 grasslands (Suyker and Verma 2001) and C_4 corn crops (Campbell *et al.* 1999). To assess the C_4 grass canopy LAI sensitivity, we doubled the LAI (from 3.75 to 7.5) in one simulation and reduced it by 33% (to 2.5) in another.

We also tested the sensitivity of our results to shade leaf temperatures, as ISOLSM does not separately calculate the energy balance of sun and shade leaves. Shade leaves can experience a very different radiation environment than sun leaves, leading to leaf temperature gradients in the canopy (Gu *et al*. 2002; Larcher 2003). Shade leaf temperatures can be lower than sun leaf temperatures during sunny days. We tested the impact of this difference on our results by setting forest shade leaf temperatures to canopy air temperatures. Finally, we assessed the sensitivity of our results to the uniform distribution of leaf nitrogen and photosynthetic capacity (V_{max}) between sun and shade leaves in ISOLSM. This uniformity could lead to larger shade leaf photosynthesis than would otherwise occur if these leaves become limited by Rubisco, which scales with leaf nitrogen. We halved V_{max} in forest shade leaves in a separate simulation.

3. Results and Analysis

We analyzed consecutive growing-season days to understand how changes in cloud cover affected the physical environment and modeled ecosystem-atmosphere CO_2 fluxes and isofluxes in a broadleaf deciduous forest canopy and a C_4 grassland canopy. Our analysis is divided into four sections to clarify the processes impacting CO_2 fluxes and isofluxes: (3.1) cloud cover effects on R_D/R_S, PAR, temperature, and humidity; (3.2) the response of photosynthesis and respiration to cloud cover; (3.3) the response of leaf and soil water $\delta^{18}O$ to cloud cover; and (3.4) the response of CO_2 isofluxes to cloud cover.

3.1 Cloud Cover Impacts on R_D/R_S and the Physical Environment

During the first three days (DOY 193-195) of the study period, the percent of the sky obscured by thick (opaque) and thin clouds was minimal (Figure 1a). During these mostly clear days, total irradiance was high, and the PAR flux was dominated by direct beam radiation except for early in the morning and early in the evening when diffuse radiation increased (Figure 1b). In this and subsequent figures, only daytime values are plotted.

These clear sky days provided a useful basis for comparison with subsequent days (DOY 196-199), which experienced increasing thick cloud cover and midday diffuse PAR irradiance, along with reduced direct and total shortwave irradiance. The peak diffuse PAR irradiance on partly cloudy days increased more than twofold from clear days. The magnitude of midday diffuse PAR irradiance was similar to direct PAR on DOY 196, and thick cloud cover exceeded 60% for several hours.). DOY 198 was by far the cloudiest day of the study period, with thick cloud cover close to 100% for much of the day (Figure 1a) and irradiance dominated by diffuse fluxes (Figure 1b). The days before and after DOY 198 were both partly cloudy, with daily maximum thick cloud cover around 60%. DOY 199 is noteworthy, as the thick and thin clouds scattered and reflected direct beam irradiance, in the process increasing the diffuse irradiance enough to produce the highest midday shortwave irradiance measured in the study period (i.e., total PAR was greater than even the clear sky days of 193, 194, and 202). This effect of unexpectedly high midday irradiance during partly cloudy periods has been observed elsewhere (Gu *et al*. 1999, 2001; Urban *et al.* 2007).

The period from DOY 200-203 was mostly clear, with the lowest cloud cover of the study period measured on DOY 202 (Figure 1a). On this day, direct beam PAR was very high, about the same peak magnitude as on the other very clear day, DOY 193, but diffuse PAR was slightly lower. DOY 204 was partly to mostly cloudy (cover greater than 80% for much of the day), and it had high diffuse PAR irradiance (Figure 1b). This day preceded a heavy rain event on DOY 205. Stratifying the days by cloud cover thus produces the following classifications: clear (sunny) days (DOY 193-195, 200-203), partly cloudy days (DOY 196-197, 199, and 204), and a cloudy day (DOY 198).

Observed relative humidity and the diffuse PAR fraction (R_D/R_S), are shown in Figure 2. (Our analysis focuses on the observed diffuse PAR fraction, which we denote with the same notation (R_D/R_S) as the diffuse shortwave fraction following Roderick 1999; although diffuse PAR and shortwave fractions can differ slightly, during our study period they were indistinguishable from one another). Diurnal profiles of relative humidity largely followed the pattern of air temperature, and R_D/R_S followed predictable patterns on clear days with higher morning and evening values (Figure 2). Midday R_D/R_S was highest on the partly cloudy and cloudy days. Notably, the partly cloudy days (DOY 196-

197, 199, and 204) did not have temperatures or humidities dramatically different from adjacent clear sky days. Modeled leaf temperatures in the forest simulation tracked measured air temperatures, though they were higher by 1-3 K on sunny days (not shown).

The increasing cloud cover during DOY 196-198 increased diffuse PAR and decreased direct and total PAR irradiance, producing a positive relationship between daytime R_D/R_S and the thick cloud cover fraction (Figure 3). Thin clouds and aerosols might also have affected R_D/R_S and contributed to some of the scatter shown in Figure 3. On partly cloudy days, midday R_D/R_S values were ~0.4, compared to ~0.15 on clear days, and the highest midday R_D/R_S occurred on DOY 198, when it reached 1.0. The strong relationship between cloud cover and R_D/R_S has been observed in a variety of other studies, and results from radiation absorption, reflection and scattering by cloud droplets.

3.2 Photosynthetic Responses to Cloud Cover Changes

3.2.1 Broadleaf Deciduous Forest

The effect of cloud cover on modeled broadleaf deciduous forest canopy photosynthesis was large. Despite the lower total PAR on partly cloudy and cloudy days (DOY 196-199, 204), simulated peak canopy photosynthesis was higher on these days than on sunny days (DOY 193-195, 200-203 – Figures 1b, 4a). This enhancement was due primarily to increases in shade leaf photosynthesis from increases in diffuse PAR on these days. There were minimal changes in modeled sun leaf photosynthesis on these days because the rate was light saturated for much of the day, and even relatively large decreases in direct PAR didn't impact sun leaf photosynthesis. During these periods, sun leaf photosynthesis was limited by the amount and capacity of the primary photosynthetic enzyme, Rubisco (i.e., Collatz *et al*. 1991). Also, the leaf temperature was slightly lower on the partly cloudy days compared to the sunny days due to lower radiant heating, thereby decreasing leaf respiration and photorespiration rates. The temperature sensitivity of the maximum carboxylation capacity (V_{max}) is important for sun leaf photosynthesis, as it is usually light saturated and depends directly on V_{max}, while photorespiration affects both light-limited and light-saturated rates (Farquhar *et al.* 1980; Collatz *et al*. 1991).

In contrast to sun leaves, forest shade leaves responded strongly to the altered radiation regime induced by clouds: as cloud cover increased, diffuse PAR and shade leaf photosynthesis increased in tandem because shade leaf photosynthesis was light limited.

On sunny days, peak shade leaf cumulative photosynthetic fluxes were less than half of sun leaf fluxes, whereas on partly cloudy and cloudy days the shade leaf fluxes equaled or exceeded the sun leaf values (Figure 4a). The overall positive simulated forest canopy photosynthetic response to increasing cloud cover (slope 0.15, $r^2 = 0.37$ - Figure 4b) thus resulted primarily from increased shade leaf carbon uptake with increased R_D/R_S.

3.2.2 C_4 Grassland

The C_4 grass canopy photosynthetic response to cloud variations was opposite that of the broadleaf deciduous forest canopy: increasing cloud cover generally led to decreased canopy photosynthesis. The negative response of C_4 photosynthesis to increasing R_D/R_S was stronger than its response to cloud cover (not shown). Although grass shade leaf photosynthesis responded positively to increased cloud cover due to increased diffuse PAR, sun leaf photosynthesis responded negatively to the decrease in direct beam radiation, and sun leaf photosynthesis was much larger than shade leaf photosynthesis during almost all cloud cover conditions (Figure 5).

The modeled C_4 grass canopy photosynthesis closely followed daily irradiance patterns, in agreement with leaf and canopy-scale observations for C_4 plants (Suyker and Verma 2001; Larcher 2003). In general, the highest predicted C_4 grass canopy photosynthesis rates occurred during the clear sky days (DOY 193-195, 200-203), and the lowest rates occurred during the cloudiest days (DOY 196, 198, 204). The one important exception (on DOY 199, which was partly cloudy) proves the rule: peak insolation values on this day were the highest of the study period due to cloud scattering and reflection, and modeled peak C_4 grass photosynthesis was also highest on this day (Figure 5a). Modeled peak canopy photosynthesis was large due to the high LAI values we imposed, although there are examples of well-watered and fertilized natural C_4 grassland and C_4 crop canopies exhibiting even higher productivity (Piedade *et al.* 1991; Jones 1992; Morison *et al.* 2000). The net ecosystem exchange (NEE) values predicted by ISOLSM (not shown) ranged from -15 to -35 μmol m^{-2} s^{-1}, similar to NEE measured in a C_4 grass-dominated pasture (Suyker and Verma 2001).

The fundamentally different response to cloud cover of the C_4 grass canopy (as opposed to the forest canopy) was at least partly due to canopy stature and the lower effective shade leaf area (and higher effective sun leaf area) in the much shorter grass canopy. Grass leaves have a more vertical orientation (erectophile morphology), and broadleaf deciduous tree leaves have a more horizontal orientation, so that at high solar angles the sun leaf area in grass canopies is higher than the comparable sun leaf area of broadleaf deciduous tree canopies (Jones 1992; Larcher 2003). Another reason for the different response to irradiance is that both sun and shade leaf photosynthetic rates are almost always limited by light in the C_4 grass simulation. A hallmark of C_4 plants is their dominance in high light and high temperature environments such as grasslands and savannas (Long *et al.* 1999; Sage *et al.* 1999). Photosynthesis in unstressed C_4 plants does not saturate on sunny days, unlike the typical light saturation for C_3 plants (Collatz *et al.* 1991, 1992).

The decline in C_4 grass canopy photosynthesis with increasing cloud cover and R_D/R_S parallels the empirical results from eddy flux studies assessed by Niyogi *et al* (2004), who found that increasing aerosol optical depth increased R_D/R_S and reduced R_S. This led to increases in net carbon uptake by C_3 ecosystems, but strong reductions in net carbon uptake for a C_4 natural grassland. Although not explicitly a response to cloud cover variations per se, this study supports our modeling results: increasing R_D/R_S and decreasing R_S reduces C_4 photosynthesis, without the diffuse light photosynthetic enhancement often seen in C_3 canopies. Our predictions also agree with Turner *et al.* (2003), who studied the relationship between measured gross primary production (GPP) and absorbed PAR in a cross-biome comparison. The C_4-dominated tallgrass prairie displayed a nearly linear relationship between GPP and APAR, unlike other biomes, which exhibited more typical light saturation responses (i.e., a hyperbolic relationship between GPP and APAR). Thus, decreases in R_S and increases in R_D/R_S, whether caused by clouds or aerosols, should decrease GPP in C_4 grasses, but not necessarily in C_3 plants.

3.2.3 Response of canopy light-use efficiency to cloud cover and R_D/R_S variations

The response of forest photosynthesis to cloud cover and irradiance is related to how efficiently the canopy converts solar radiation to chemical energy, a quantity referred to as gross or GPP light-use efficiency (LUE - mol CO_2 mol^{-1} APAR). The broadleaf deciduous forest gross LUE was inversely proportional to irradiance. Indeed, the forest canopy strongly increased its gross LUE as R_D/R_S increased (Figure 6a). The daily averaged forest gross LUE for clear/sunny days (DOY 193-195, 200-203) was 0.031 mol

CO_2 mol^{-1} APAR, for partly cloud days (DOY 196-197, 199, 204) was 0.038 mol CO_2 mol^{-1} APAR, and for the cloudy day (DOY 198) was 0.048 mol CO_2 mol^{-1} APAR. This pattern follows the expectations of increasing LUE with increasing cloud cover and R_D/R_S demonstrated previously in eddy flux (e.g., Hollinger *et al*. 1994; Gu *et al*. 2002; Rocha *et al.* 2004; Min 2005) and modeling (Norman and Arkebaur 1991; Choudhury 2001) studies. The increase of LUE with R_D/R_S depends on canopy structure and openness (Alton *et al.* 2005), and, as we show below, on photosynthetic pathway.

During periods of high R_D/R_S, both sun and shade leaves in the forest were light limited and thus displayed a linear response to APAR. The linear slope between photosynthesis and APAR is defined as the quantum yield of photosynthesis (Larcher 2003). In C_3 plants the highest intrinsic quantum yield is ~0.085 mol CO_2 mol^{-1} incident PAR, and its temperature sensitivity is largely driven by photorespiration (Collatz *et al*. 1998; Ehleringer *et al*. 1997). Therefore, canopy LUE under low light closely follows the temperature-dependent photorespiration rate. Forest LUE values reached their lowest values around midday when sun leaves were light saturated and leaf temperatures were high. Forest canopy LUE dropped non-linearly with temperature and reached its lowest values on the sunniest, hottest days when R_D/R_S was lowest (not shown).

The C_4 canopy maintained high gross LUE over the study period, and was relatively insensitive to variations in cloud cover, irradiance, and leaf temperature. Since C_4 sun and shade leaf photosynthesis was almost always light limited, the relationship between canopy photosynthesis and APAR was linear across the entire PAR range, and thus canopy LUE was very close to the leaf quantum yield. The intrinsic modeled leaf C_4 quantum yield is 0.06 mol CO_2 mol^{-1} incident PAR (Collatz *et al*. 1998), although natural C_4 monocots can occasionally exceed this value (Ehleringer *et al*. 1997). C_4 plants typically maintain nearly constant quantum yields across a range of temperatures under low light conditions (Ehleringer *et al*. 1997; Collatz *et al.* 1998). During most daytime hours of the study period, the C_4 grass canopy LUE varied from ~0.035-0.05 mol CO_2 mol^{-1} APAR, and, unlike the forest canopy, there was no consistent relationship with cloud cover or leaf temperature. There was a relationship with R_D/R_S, although it was weak compared with the forest LUE response to R_D/R_S (Figures 6a,b).

3.3 Leaf and Soil Water $\delta^{18}O$ Responses to Cloud Cover Changes

The simplest formulation for leaf water $\delta^{18}O$ is captured in the steady-state prediction for $\delta^{18}O$ of an evaporating surface, in this case within leaves (Craig and Gordon 1965; Farquhar *et al.* 1989; Yakir and Sternberg 2000):

$$\delta^{18}O_{lws} = \delta^{18}O_{xy} + \varepsilon_k + \varepsilon^* + \left(\delta^{18}O_{cv} - \varepsilon_k - \delta^{18}O_{xy}\right)\frac{e_a}{e_i} \qquad (1).$$

In this equation, $\delta^{18}O_{xy}$ and $\delta^{18}O_{cv}$ are the $^{18}O/^{16}O$ composition of stem xylem (source) water and within-canopy atmospheric water vapor; ε_k is the weighted mean of kinetic fractionations against $H_2^{18}O$ molecules diffusing through the stomata and across the leaf boundary layer (32 and 21‰, respectively – Cappa *et al.* 2003); ε^* is the equilibrium fractionation between liquid and vapor phases over a saturated surface (~9.4‰ at 298K – Horita and Wesolowski 1994); and e_a and e_i are the water vapor pressures (Pa) in the canopy atmosphere and inside leaf stomata, respectively.

Bulk leaf water $\delta^{18}O$ is often not accurately represented by a steady-state formulation (Dongmann *et al.* 1974; Zundel *et al.* 1978; Wang *et al.*1998; Harwood *et al.* 1998; Cernusak *et al.* 2002; Cuntz *et al*. 2003a; Barbour *et al.* 2004; Farquhar and Cernusak 2005; Cernusak *et al.* 2005; Seibt *et al.* 2006). Dongmann *et al.* (1974) first proposed a non-steady state leaf water model; our treatment in ISOLSM follows closely from their work, and describes the change in leaf water $\delta^{18}O$ as an asymptotic approach to a steady-state value. The non-steady-state leaf water $\delta^{18}O$ at time *t* (i.e., $\delta^{18}O_{lw}(t)$) is calculated implicitly from the steady-state estimate ($\delta^{18}O_{lws}(t)$) and the non-steady-state $\delta^{18}O_{lw}$ (i.e., $\delta^{18}O_{lw}(t-1)$) from the previous time step as follows:

$$\delta^{18}O_{lw}(t) = e^{\frac{-\Delta t}{\tau}}\delta^{18}O_{lw}(t-1) + \left(1 - e^{\frac{-\Delta t}{\tau}}\right)\delta^{18}O_{lws}(t) \qquad (2).$$

Here, τ is the leaf water time constant (s) and in practice Δt is the model time step (s). τ is calculated separately for sun and shade leaves as the ratio between the leaf stock of water interacting with transpiration (M_l) and the gross water vapor flux out of leaves:

$$\tau = \frac{M_l}{\left(\frac{e_i}{RT_v}\right)g_s} \qquad (3).$$

Here, R is the universal gas constant (8.314 J mol^{-1} K^{-1}), T_v is vegetation temperature (K), and g_s is stomatal conductance (sun or shade leaf, m s^{-1}). The leaf water content, M_l, of both sun and shade leaves is set to a constant value of 10 mol m^{-2}, which is consistent with limited available observations from a temperate needleleaf forest (Seibt *et al.* 2006) and a tropical broadleaf forest (Förstel 1978). In reality, the water content of the average shade leaf is undoubtedly different from the average sun leaf, since there are well-known differences in specific leaf area between sun and shade leaves (Chapin *et al*. 2002; Larcher 2003). However, we lacked data to reliably and accurately set this difference and assumed a constant value in both biomes and leaf types.

3.3.1 Broadleaf Deciduous Forest

Simulated non-steady $\delta^{18}O_{lw}$ for forest sun and shade leaves varied by over 20‰ during the study period (Figure 7a - all δ^{18}O-H_2O values are reported relative to the V-SMOW scale). The diurnal cycle of $\delta^{18}O_{lw}$ for sun and shade leaves was inversely related to canopy relative humidity. Assuming steady state and no leaf boundary layer fractionation, the change in δ^{18}O of an evaporating leaf at steady state will be roughly -0.4‰ for each percent change in relative humidity (Craig and Gordon 1965). This slope will be slightly smaller when including isotopic fractionation across the leaf boundary layer and non-steady-state effects. Over the study period, the slope of the linear regression for daytime sun leaf $\delta^{18}O_{lw}$ versus canopy relative humidity was -0.39‰ per % change in relative humidity. By contrast, the slope for shade leaves was lower, approximately -0.28‰ per % change in relative humidity. $\delta^{18}O_{cv}$ varied diurnally between -13‰ and -16‰ in response to canopy transpiration, soil evaporation, and exchange with above-canopy air. This variation was dampened by a 3-hour canopy turnover time imposed to account for turbulent air mass exchange between the canopy and atmosphere (Riley *et al*. 2002).

The sun and shade $\delta^{18}O_{lw}$ differed from the steady-state ($\delta^{18}O_{lws}$) and from each other during most of the day (both leaves had the same water content, were at the same temperature, and were exposed to the same canopy vapor pressure and isotopic composition). This difference occurs because the leaf water time constant depends on the stomatal conductance of each leaf type (equation 3), which is linked to the photosynthetic rate. For much of the day, sun leaf $\delta^{18}O_{lw}$ was close to steady state. Shade leaf $\delta^{18}O_{lw}$

generally lagged sun leaf $\delta^{18}O_{lw}$, with smaller lags on partly cloudy and cloudy days when shade leaf photosynthesis and transpiration were higher due to enhanced diffuse PAR (e.g., DOY 196, 204). Both sun and shade leaves remained elevated above source stem water, especially in the early evening and through much of the night.

As is apparent from $\delta^{18}O_{xy}$ (Figure 7a), variation in modeled soil water δ^{18}O ($\delta^{18}O_{sw}$) was minimal across the study period. Even in the upper soil layers where $\delta^{18}O_{sw}$ can strongly increase due to evaporative enrichment (Allison *et al.* 1983; Riley 2005), $\delta^{18}O_{sw}$ did not vary greatly because transpiration dominated evapotranspiration in these high LAI simulations. The magnitude and variability of soil-respired CO_2 isofluxes was fairly minimal, in agreement with earlier Great Plains modeling studies (Riley *et al.* 2002, 2003; Lai *et al.* 2005; Still *et al.* 2005), and will not be discussed further.

3.3.2 C_4 Grassland

There was an unanticipated difference between the broadleaf forest and C_4 grassland $\delta^{18}O_{lw}$, with peak C_4 grassland $\delta^{18}O_{lw}$ over the period never exceeding 12‰, whereas peak forest $\delta^{18}O_{lw}$ routinely exceeded 18‰ (Figure 7a,b), despite identical precipitation δ^{18}O, radiation, and meteorological forcing (including above-canopy relative humidity). The difference is due to feedbacks between transpiration and within-canopy relative humidity. The canopy relative humidity (not shown) was substantially higher in the C_4 grassland. Canopy relative humidity is calculated in ISOLSM from the canopy temperature and vapor pressure, which depends on exchanges with background vapor pressure, as well as transpiration and soil and canopy evaporation. The canopy relative humidity in the C_4 grassland simulation never dropped below 55% over the study period, whereas modeled canopy relative humidity in the broadleaf forest was only slightly elevated from the measured above-canopy humidity, reaching values below 40% near midday. The higher average daytime relative humidity in the C_4 canopy (relative to the broadleaf forest canopy) depleted $\delta^{18}O_{lw}$.

The higher relative humidity in the C_4 canopy was due to higher transpiration fluxes. Although C_4 plants typically exhibit water-use efficiencies roughly twice those of comparable C_3 plants (Pearcy and Ehleringer 1984), this difference was overcome by much higher photosynthetic fluxes in the C_4 grass canopy compared to the forest canopy (Figures 4a, 5). The higher relative humidity in the C_4 grass canopy was also due to a lower aerodynamic conductance between the grass canopy and overlying atmosphere compared to the taller and aerodynamically rougher forest, leading to a greater offset between the canopy relative humidity and the background atmosphere. The effect of these differences is also apparent in the greater diurnal cycle of canopy vapor $\delta^{18}O$ ($\delta^{18}O_{cv}$) in the C_4 grassland (Figure 7b), as it was more strongly influenced by transpiration. The greater diurnal cycle in $\delta^{18}O_{cv}$ also contributed to the transpiration feedback on $\delta^{18}O_{lw}$, although the feedback was primarily due to the change in canopy relative humidity.

3.4 Response of Photosynthetic Isofluxes to Cloud Cover and R_D/R_S

Leaf CO_2 isofluxes depend on both photosynthesis and discrimination against $CO^{18}O$. Discrimination against $CO^{18}O$ (${}^{18}\Delta$) depends upon the $\delta^{18}O$ value of CO_2 in equilibrium with H_2O inside leaf chloroplasts ($\delta^{18}O_c$) and the ratio of chloroplast CO_2 to atmospheric CO_2 concentrations (C_c/C_a). Gaseous CO_2 equilibrates with liquid water in the mesophyll cells lining the bottom of the stomatal pore via the activity of the carbonic anhydrase enzyme. This equilibration labels CO_2 with the isotopic signature of leaf water plus an equilibrium offset (Farquhar and Lloyd 1993; Farquhar et al. 1993; Gillon and Yakir 2000; Affek *et al*. 2005), and has been shown to be lower in C4 grasses (Gillon and Yakir 2001). The discrimination can be estimated as (Farquhar and Lloyd 1993; Farquhar *et al.* 1993; Ciais *et al.*1997a; Gillon and Yakir 2000; Yakir and Sternberg 2000):

$$^{18}\Delta = \varepsilon_d + \frac{C_c}{C_a - C_c}\left(\delta^{18}O_c - \delta^{18}O_a\right) \qquad (4).$$

ε_d is the weighted kinetic fractionation accompanying diffusion of $CO^{18}O$ molecules across the stomata, boundary layer, and the mesophyll walls (~7.4‰ - Farquhar and Lloyd 1993; Gillon and Yakir 2001), $\delta^{18}O_c$ is calculated from $\delta^{18}O_{lw}$ and a temperature-dependent fractionation factor (Brenninkmeier *et al*. 1983), and $\delta^{18}O_a$ is the $\delta^{18}O$ value of background atmospheric CO_2. The $\frac{C_c}{C_a - C_c}$ term arises from mass balance of $CO^{18}O$ molecules, and when multiplied by net leaf uptake, quantifies the back- or retro-diffusion flux of CO_2 molecules, which have a different $\delta^{18}O$ from when they entered the leaf. This change occurs because only some of the CO_2 entering the leaf is fixed by photosynthesis, while the remainder diffuses out after full or partial isotopic equilibration with leaf water (Farquhar *et al.* 1993; Flanagan *et al*. 1994; Gillon and Yakir 2001).

These bi-directional fluxes, termed F_{al} (atmosphere-to-leaf) and F_{la} (leaf-to-atmosphere), together sum to net photosynthesis, A_{net} (which includes leaf respiration). Each of these global fluxes (roughly 300 and 200 Pg C yr^{-1} for F_{al} and F_{la}, respectively – Ciais *et al.* 1997a) is larger than any other carbon flux term in the contemporary carbon budget. Equation 4 can be recast as a function of F_{al} and F_{la}:

$$^{18}\Delta = \frac{F_{la}}{A_{net}}\left(\delta^{18}O_c - \varepsilon_d - \delta^{18}O_a\right) + \frac{F_{al}}{A_{net}}\varepsilon_d \qquad (5).$$

The first, right-hand side term captures the effective discrimination associated with the return, or retro-diffused, flux from leaves, and its sign and magnitude vary directly with changes in $\delta^{18}O_c$. The combined net photosynthetic isoflux, in units of μmol ‰ m^{-2} s^{-1}, is the product of photosynthetic discrimination ($^{18}\Delta$) and net leaf photosynthesis (A_{net}):

$$A_{net}{}^{18}\Delta = F_{la}\left(\delta^{18}O_c - \varepsilon_d - \delta^{18}O_a\right) + F_{al}\varepsilon_d = {}^{18}F_{la} + {}^{18}F_{al} \qquad (6).$$

Bi-directional CO_2 isofluxes across leaf stomata can occur during nighttime periods (e.g., Cernusak *et al.* 2004; Barbour *et al.* 2007). Although this effect is potentially important, accurate quantification requires a model with a canopy air space and prognostic calculations of CO_2 and $CO^{18}O$ concentrations throughout the night (e.g., Seibt *et al.* 2006), along with a model that accurately predicts stomatal conductance and the concentration of CO_2 in the sub-stomatal air spaces (C_i) and inside leaf chloroplasts (C_c) when photosynthesis is zero. For this study, we focused on daytime isofluxes only.

3.4.1 Broadleaf Deciduous Forest

The $^{18}\Delta$ diurnal cycle (not shown) was strongly related to $\delta^{18}O_{lw}$ enrichment as canopy relative humidity declined with increasing air temperature. There was a decline in $^{18}\Delta$ with increasing cloud cover that followed from a small decrease in $\delta^{18}O_{lw}$ on partly cloudy days, and a large decrease in $\delta^{18}O_{lw}$ on the cloudy day (Figures 1a, 7a). Neither C_c nor leaf temperature (the other components of $^{18}\Delta$) varied appreciably with cloud cover for either leaf type. The bi-directional leaf CO_2 fluxes, F_{al} and F_{la}, varied diurnally with photosynthesis and increased strongly with cloud cover, particularly for shade leaves.

The ${}^{18}F_{al}$ and ${}^{18}F_{la}$ isofluxes were often in opposition: the gross flux into stomata (${}^{18}F_{al}$) always enriched atmospheric $\delta^{18}O_a$ (i.e., was always positive in δ–notation), whereas the retro-diffused flux (${}^{18}F_{la}$) depleted $\delta^{18}O_a$ in the morning (i.e., a negative isoflux) and enriched it in the afternoon (Figure 8a). The early morning depletion occurred because $\delta^{18}O_{lw}$ (and thus $\delta^{18}O_c$) was relatively depleted from the previous night when it approached $\delta^{18}O_{xy}$ (Figure 7a); also, early morning canopy relative humidity was still high, and the transpiration flux was reduced due to low light levels, thus affecting the leaf water time constant. At this site, where we imposed a fixed $\delta^{18}O_a$ consistent with the measured annual zonal mean (-0.5‰), $\delta^{18}O_c$ must exceed ~7.0‰ before the retro-diffused isoflux (${}^{18}F_{la}$) has a positive isotopic forcing (i.e., enriches $\delta^{18}O_a$).

As relative humidity decreased in the late morning, $\delta^{18}O_c$ became more enriched until it exceeded the ~7‰ threshold and the leaf-to-atmosphere isoflux (${}^{18}F_{la}$) reinforced the atmosphere-to-leaf isoflux (${}^{18}F_{al}$). The forest sun leaf $\delta^{18}O_{lw}$ corresponding to this $\delta^{18}O_c$ threshold occurred at a canopy relative humidity of ~60%. Only on the cloudiest and coolest day (DOY 198) did $\delta^{18}O_{lw}$ stay below this value throughout the day (Figures 7a, 8a). The greatest $\delta^{18}O_{lw}$ enrichment occurred on the sunniest, hottest day when canopy relative humidity was lowest (DOY 202), and ${}^{18}F_{la}$ was mostly positive. Due to high leaf temperatures on DOY 202, however, A_{net} and net leaf isofluxes ($A_{net}{}^{18}\Delta$ or ${}^{18}F_{al}$ + ${}^{18}F_{la}$) were lowest of the study period.

If $\delta^{18}O_{lw}$ and $\delta^{18}O_c$ are sufficiently negative, the net leaf isoflux can deplete $\delta^{18}O_a$. The $\delta^{18}O_c$ where negative net photosynthetic isotope fluxes (${}^{18}F_{al} + {}^{18}F_{la} < 0$) occur is a function of $\delta^{18}O_a$, the C_c/C_a ratio, and ε_d. $\delta^{18}O_c$ values more depleted than approximately -4.2‰ caused net forest photosynthetic isofluxes to be negative. During the 12-day study period, negative CO_2 isofluxes occurred only briefly on DOY 193 when $\delta^{18}O_{lw}$ approached $\delta^{18}O_{xy}$ and photosynthesis was just beginning (Figure 8a). Because the $\delta^{18}O$ of growing-season precipitation is rarely more depleted than -5‰ at these latitudes (Welker 2000; Bowen and Wilkinson 2002), forest photosynthetic isofluxes will almost always enrich $\delta^{18}O_a$. At higher latitudes where precipitation $\delta^{18}O$ is lower, leaf CO_2 isofluxes can deplete $\delta^{18}O_a$ (e.g., Francey and Tans 1987; Farquhar et al. 1993; Ciais *et al*. 1997b), due to ${}^{18}F_{la}$ outweighing ${}^{18}F_{al}$.

The net photosynthetic isoflux ($A_{net}{}^{18}\Delta$, solid line in Figure 8a) generally followed the daily variations in canopy photosynthesis (Figure 4a), with larger isofluxes on partly cloudy days (DOY 196-197, 199, 204) than on clear, sunny days (DOY 193-195, 201-203), an effect driven by shade leaves. However, the cloudy day (DOY 198) exhibited intermediate CO_2 isofluxes: although it had the largest peak photosynthesis, this was countered by the lowest $\delta^{18}O_{lw}$ and ${}^{18}\Delta$ of the study period (Figures 4a, 7a, 8a). Partitioning the net leaf isoflux ($A_{net}{}^{18}\Delta$) into ${}^{18}F_{al}$ and ${}^{18}F_{la}$ (equation 6) reveals the canopy response to cloud cover in more detail. The ${}^{18}F_{al}$ isoflux increased strongly with increasing cloud cover due to an increase in shade leaf and canopy photosynthesis with cloud cover. By contrast, ${}^{18}F_{la}$ did not exhibit a strong relationship with cloud cover during daytime hours of the study period. Indeed, both negative and positive ${}^{18}F_{la}$ values occurred for a range of cloud cover, as $\delta^{18}O_{lw}$ and thus $\delta^{18}O_c$ alternated from relatively depleted values in the morning to enriched values in the afternoon after they crossed the ~7.0‰ threshold. Thus, for the sum of ${}^{18}F_{al}$ and ${}^{18}F_{la}$ (i.e., $A_{net}{}^{18}\Delta$), no clear response to cloud cover occurred. When net photosynthetic isofluxes are plotted against R_D/R_S, however, there was a weak negative relationship, with the highest isofluxes centered at an R_D of ~0.4. This was driven by ${}^{18}F_{la}$, which peaked around this value in our simulations; at R_D/R_S values above ~0.6, ${}^{18}F_{la}$ was always negative. The peak isoflux at an R_D/R_S of 0.4 was not driven solely by photosynthetic responses to diffuse irradiance, as peak canopy photosynthesis occurred at higher R_D/R_S values. Rather, it was the combination of enhanced photosynthesis with higher $\delta^{18}O_{lw}$ due to lower canopy relative humidity at this particular R_D/R_S. These conditions occurred around midday on the partly cloudy days (DOY 196, 199, 204) that have the largest peak and cumulative daily isofluxes.

3.4.2 C_4 Grassland

There were large differences in leaf isofluxes between the forest and C_4 grassland simulations that arose from differences in the internal CO_2 concentrations between these different physiological types, as well as differences in their $\delta^{18}O_c$ values (section 3.3). Comparing chloroplast CO_2 concentrations between C_3 and C_4 plants is difficult since the C_4 pathway concentrates CO_2 around Rubisco in the bundle sheath cell chloroplasts, and raises CO_2 concentrations to much higher levels than occur in mesophyll cell chloroplasts of C_3 plants (von Caemmerer and Furbank 2003). For these simulations, we used the C_4

C_i value calculated in ISOLSM. Typical C_i/C_a ratios for C_4 plants range from 0.2-0.4, whereas those for most C_3 plants are 0.6-0.8 (Pearcy and Ehleringer 1984; Collatz *et al.* 1991, 1992). At similar photosynthetic rates, F_{la} can be much higher in C_3 than C_4 plants (Still *et al.* 2005; Hoag *et al.* 2005). For example, a C_i/C_a ratio of 0.8 produces a F_{la} four times larger than a ratio of 0.2 produces for the same net leaf flux.

The C_4 grass photosynthetic isoflux, dominated by ${}^{18}F_{al}$ from sun leaves, is almost always larger and less variable than the forest isoflux (Figure 8b). However, ${}^{18}F_{la}$ is smaller in the grass than in the forest, and it remains negative throughout the day and never reinforces ${}^{18}F_{al}$, except for three brief periods on DOY 199, 203, and 204 (Figure 8a,b). This negative isotopic forcing on the atmosphere is due to the lower $\delta^{18}O_{lw}$ (Figure 7a,b) and the larger ε_d in the C_4 grass simulation. $\delta^{18}O_c$ must exceed a threshold value of ~7.9‰ before the C_4 ${}^{18}F_{la}$ has a positive isotopic forcing on the atmosphere. Because leaf temperatures exceeded 30˚C on the days with highest $\delta^{18}O_{lw}$ (DOY 199, 200, 202), and the CO_2-H_2O fractionation has a sensitivity of -0.2‰ K^{-1} (Brenninkmeier *et al.* 1983; Ciais *et al.* 1997a), ${}^{18}F_{la}$ is almost always negative during the study period (Figure 8b).

Because the magnitude of ${}^{18}F_{la}$ will be much smaller in C_4 plants compared to C_3 plants due to lower C_i/C_a ratios (Still *et al.* 2005) and reduced equilibration between CO_2 and H_2O from lower carbonic anhydrase activity (Gillon and Yakir 2001), photosynthesis by C_4 plants will almost always enrich $\delta^{18}O_a$. The positive isotopic forcing associated with ${}^{18}F_{al}$ will in almost every case be much larger than the negative isotopic forcing from ${}^{18}F_{la}$. Because C_4 plants are largely restricted to tropical and subtropical savannas and grasslands (Still *et al.* 2003), the $\delta^{18}O$ of precipitation and thus of plant xylem water ($\delta^{18}O_{xy}$), is relatively enriched (Bowen and Wilkinson 2002). For example, Ometto *et al.* (2005) measured Amazonian C_4 pasture grasses with $\delta^{18}O_{xy}$ values between -3‰ and -9‰, and mean values around -5‰. These values, and measurements from C_4-dominated tallgrass prairies in Oklahoma and Kansas (Helliker *et al.* 2002; Riley *et al.* 2003; Lai *et al.* 2006), are similar to the mean predicted $\delta^{18}O_{xy}$ at our site (Figure 7). Given a typical midday C_4 plant C_i/C_a ratio of 0.3 and assuming complete equilibration, $\delta^{18}O_c$ at this site would have to be below approximately -17.3‰ for net C_4 photosynthetic isofluxes to deplete $\delta^{18}O_a$. Using precipitation $\delta^{18}O$ regressions from Bowen and Wilkinson (2002),

$\delta^{18}O_{lw}$ and thus $\delta^{18}O_c$ values that are sufficiently depleted occur above ~60°N. Although C_4 plants do grow north of 50° N (e.g., Schwarz and Redmann 1988; Beale and Long 1995), they are uncommon and do not substantially affect regional carbon fluxes.

While C_4 canopy photosynthesis decreased slightly with increasing cloud cover, net photosynthetic isofluxes ($A_{net}{}^{18}\Delta$) exhibited no clear relationship with cloud cover. ${}^{18}\Delta$ did not vary with cloud cover, as an increase in the F_{al} component of ${}^{18}\Delta$ due to an increase in C_c with cloud cover was countered by a decrease in the F_{la} component of ${}^{18}\Delta$ driven by the slight decrease of $\delta^{18}O_{lw}$ and $\delta^{18}O_c$ with cloud cover. Over the study period, the flux-weighted mean C_4 grassland canopy ${}^{18}\Delta$ was ~12‰, with ~2/3 of this from ε_d. There was a weak negative response of $A_{net}{}^{18}\Delta$ to increasing R_D/R_S, just as there was between C_4 canopy photosynthesis and R_D/R_S. In both cases, peak uptake occurred at R_D/R_S values between 0.2 and 0.4, and declined sharply above 0.4. There was a strong positive relationship (slope = 0.46; r^2 = 0.89) between the net C_4 photosynthetic isoflux and incident PAR (i.e., the canopy isotope light response curve - Figure 9).

3.5 Sensitivity to Leaf Area Index

3.5.1 Broadleaf Deciduous Forest

We examined the sensitivity of our results to LAI given the importance of this canopy characteristic in the response to clouds and R_D/R_S as highlighted by earlier studies (e.g., Rocha *et al.* 2004; Urban *et al.* 2007; Knohl and Baldocchi 2008). We altered LAI values throughout the study period, with other model driving data unchanged from control simulations. Relative to the control, forest canopy photosynthesis and transpiration declined in the low LAI simulation and increased in the high LAI one, driven by the shade leaf response. The changes in canopy transpiration lowered or raised canopy relative humidity by a few percent relative to the base case. The impact of changing LAI on canopy relative humidity and $\delta^{18}O_{lw}$ was most dramatic on the cloudy day (DOY 198) when R_D/R_S and diffuse PAR were highest. This day exhibited the highest peak shade leaf and canopy photosynthesis in the base LAI simulation, and also the greatest humidification of the canopy from transpiration (since wind speed and exchange with the atmosphere was not different from adjacent days). On DOY 198, peak daytime steady-state $\delta^{18}O_{lw}$ values were raised by 1.4‰ in the low (3.5) LAI simulation relative to the base case, and lowered by 0.3‰ in the high (6.5) LAI simulation.

Taken in isolation, this transpiration feedback on $\delta^{18}O_{lw}$ would increase (decrease) $^{18}\Delta$ in the lower (higher) LAI simulations. However, the retroflux scalar (equation 4) was lowered in the reduced LAI simulation as the relative contribution of shade leaves with slightly higher C_c values declined relative to the base LAI. The effect of these differences was to quantitatively reduce the importance of $^{18}F_{la}$ in the reduced LAI simulations, and as a result, net photosynthetic isofluxes ($A_{net}{}^{18}\Delta$) were more dominated by $^{18}F_{al}$. Because $^{18}F_{al}$ scales with leaf photosynthesis and is unaffected by $\delta^{18}O_{lw}$, it exhibited a positive correlation with cloud cover; as LAI was reduced, a coherent relationship between $A_{net}{}^{18}\Delta$ and cloud cover emerged. Indeed, in the low LAI simulation, net photosynthetic isofluxes on DOY 198 reached higher peak values than on the partly cloudy days (DOY 196, 199, 204) that had the highest isofluxes in the base LAI case (Figure 10). This resulted from a combination of enhanced shade leaf photosynthesis and enriched $\delta^{18}O_{lw}$ due to a reduced transpiration feedback on canopy relative humidity. $\delta^{18}O_{lw}$ and $\delta^{18}O_c$ were even high enough on DOY 198 in the low LAI simulation to briefly surpass the ~7.0‰ forest threshold (section 3.4.1), and $^{18}F_{la}$ reinforced $^{18}F_{al}$ to enrich $\delta^{18}O_a$ (Figure 10).

3.5.2 C_4 Grassland

We also assessed the sensitivity to LAI in the C_4 grass canopy, with other driving variables held constant. For these simulations, we decreased the LAI from the base case by one-third (to a LAI of 2.5) and increased it two-fold (to a LAI of 7.5). The reduced LAI lowered canopy photosynthesis and transpiration in the C_4 grassland relative to the base case. The expected response led to several changes that modified photosynthetic isofluxes, primarily via the same transpiration feedback on canopy relative humidity and $\delta^{18}O_{lw}$ that was found for the forest simulations. In particular, $\delta^{18}O_{lw}$ values increased in the reduced LAI simulations as the transpiration flux was lowered and the canopy relative humidity more closely tracked the observed, above-canopy humidity shown in Figure 2. Unlike the forest simulations, reducing LAI did not strengthen the relationship between leaf isofluxes and cloud cover. The negative response of C_4 photosynthesis to increasing cloud cover and R_D/R_S was similar for the different LAI values, and the isotope light response curve remained linear in all LAI simulations (Figure 9).

4. Discussion and conclusions

Terrestrial ecosystems are likely to respond to changes in irradiance, temperature, relative humidity, and R_D/R_S driven by changes in cloud cover. For example, Min and Wang (2008) showed that interannual cloud cover variations drive interannual carbon fluxes in a temperate broadleaf forest. Clouds influence other ecological proceses like shoot growth and reproduction (Graham *et al*. 2003), photosynthesis of understory species (Johnson and Smith 2006, 2008), tree growth (Williams *et al.* 2008), and range boundaries (Fischer *et al*. in press). At the leaf scale, diffuse light is used less efficiently for photosynthesis than direct light (Brodersen *et al*. 2008), whereas at the canopy-scale, the opposite response is observed. Yakir and Israeli (1995) documented how artificially reducing irradiance reduced growth but increased ^{13}C discrimination in an experimental plantation; this result is buttressed by work showing that increasing R_D/R_S in a multi-layer canopy model increases Ci/Ca and ^{13}C discrimination (Knohl and Baldocchi 2008).

Our results illustrate the myriad impacts that clouds have on biosphere-atmosphere $CO^{18}O$ exchanges. We examined a sequence of mid-summer days in which the light intercepted by the canopy varied from irradiance dominated by direct beam radiation (sunny) to days with high total irradiance but an increasing diffuse fraction (partly cloudy) to days in which almost all irradiance was diffuse (cloudy). This variation allowed a detailed examination of the mechanisms that drive ecosystem isotopic states and exchanges, and to explore how ecological properties influence the mechanisms and responses. Although this study only examined a portion of the growing season, we can hypothesize that, when integrated to a larger scale, clouds have a substantial impact on biosphere-atmosphere $CO^{18}O$ exchanges through their varied impacts on direct and diffuse radiation, leaf temperature, relative humidity, leaf water enrichment, and bi-directional leaf fluxes (F_{al} and F_{la}). These effects vary strongly with canopy structure, LAI, precipitation δ^{18}O, and photosynthetic pathway.

The forest canopy increased photosynthesis with increasing cloud cover and R_D/R_S, whereas the C_4 grass canopy exhibited a negative response to both increasing cloud cover and R_D/R_S. The LUE of the forest canopy was strongly related to R_D and leaf temperature, whereas the grass canopy LUE was relatively insensitive to environmental conditions.

Compared to sunny conditions, the forest canopy exhibited larger photosynthetic isofluxes on partly cloudy days. The response of forest leaf isofluxes to cloud cover depends strongly on LAI, primarily via a feedback of transpiration on canopy relative humidity and $\delta^{18}O_{lw}$. Whereas the relationship between forest canopy photosynthesis and cloud cover (i.e., Figure 4b) became stronger with increasing LAI, the relationship between canopy photosynthetic isofluxes ($A_{net}{}^{18}\Delta$) and cloud cover weakened with increasing LAI.

In contrast, photosynthesis and isofluxes in the C_4 grass canopy declined with increasing cloud cover and R_D/R_S, regardless of LAI. This opposite response resulted primarily from the lower effective shade leaf LAI in the lower stature grass canopy compared to the broadleaf forest, as well as the near-constant light limitation on photosynthesis in C_4 sun and shade leaves. These different responses represent a fundamental functional distinction between these globally important vegetation types.

It is important to acknowledge some of the modeling limitations in the work reported here. One deficiency is the lack of a separate energy balance and leaf temperature calculation for shade leaves. High LAI values are not uncommon in many forests, and the fraction of canopy photosynthesis attributable to shade leaves increases with LAI. An incorrect shade leaf temperature will impact canopy $CO^{18}O$ exchanges in several ways. First, $\delta^{18}O_{lw}$ is sensitive to leaf temperature because of its impact on the saturation vapor pressure inside leaves. Second, each 1°C increase in leaf temperature reduces the equilibrium liquid-vapor fractionation by ~0.07‰ for typical ambient temperatures (Horita and Wesolowski 1994), and also reduces the equilibration fractionation between CO_2 and H_2O by -0.2‰ (Brenninkmeier *et al*. 1983). Leaf temperature also influences the leaf surface relative humidity and stomatal conductance, which in turn impacts C_i and bi-directional CO_2 fluxes across stomata. Finally, leaf temperature affects photosynthesis and respiration (Collatz *et al*. 1991, 1992). However, we tested the sensitivity of our results by varying shade leaf temperature and found the impact to be small (not shown).

We also tested the impact of varying photosynthetic capacity (V_{max}) between sun and shade leaves. When we halved shade leaf V_{max} in the forest simulation, there was no change in shade leaf or total canopy photosynthesis, simply because shade leaf photosynthesis is always light limited. This prediction confirms the results of Leuning *et* *al.* (1995), who showed with a multi-layer canopy model that total photosynthesis of shaded leaves is insensitive to the nitrogen distribution within a canopy. And, as shown by de Pury and Farquhar (1997), even with nitrogen and photosynthetic capacity distributed between sun and shade leaves as a function of optical depth in the canopy, the photosynthetic rate of shade leaves is always limited by light (i.e., by electron transport rate) and not by Rubisco.

We contend that these model limitations have small impacts on our conclusions. One could test this assumption by conducting similar site-scale analyses with a one-dimensional, multi-layer canopy models that also included turbulent transport and leaf nitrogen variations within the canopy (e.g., Baldocchi and Bowling 2003; Knohl and Baldocchi 2008). However, for predictions of the impact of cloudiness on ecosystem-atmosphere $CO^{18}O$ exchanges at regional to global scales, a sun/shade model like ISOLSM that has already been integrated into global climate models (Noone *et al.* 2004; Buenning *et al., in prep*) is preferable for computational reasons.

Although the differences in the response to cloudiness between C_3 and C_4 vegetation is largely due to differing F_{al} and F_{la} and photosynthetic rates, there are additional physiological and anatomical differences that would further impact $CO^{18}O$ exchanges that we did not consider. The differences between forest and grassland isofluxes would have been even larger if we had reduced the C_4 grass carbonic anhydrase activity (Gillon and Yakir 2001). For the work presented here we assumed complete equilibration between CO_2 and $\delta^{18}O_{lw}$ for both vegetation types, as we were interested primarily in ecosystem responses to changes in cloud cover as mediated by canopy structure and photosynthetic pathway. Also, we lacked field data on equilibration in this region, and recent studies suggest conflicting results for assigning appropriate values in modeling studies. Gillon and Yakir (2001) suggest a mean equilibration value of 0.4 for C_4 grasses; recent work with C_4 corn plants suggests values closer to C_3 plants (Affek *et al.* 2005). Laboratory measurements with both wild-type and transgenic individuals of a C_4 dicot also suggest higher values from *in vitro* carbonic anhydrase assays (Cousins *et al.* 2006). Moreover, a recent phylogenetic analysis suggests that reduced carbonic anhydrase activity may not be simply a trait of grasses with the C_4 photosynthetic pathway, but may be more widespread among tropical grass lineages, including several widespread and productive C_3 grass species (Edwards *et al.* 2007). We also did not consider the large $\delta^{18}O_{lw}$ enrichment observed along leaf veins of C_4 grasses (Helliker and Ehleringer 2000), which can affect leaf $CO^{18}O$ fluxes.

This study demonstrates the complex responses of terrestrial ecosystems to changes in cloud cover, particularly with respect to oxygen isotope fluxes of CO_2. The broadleaf forest and C_4 grassland are predicted to have fundamentally different responses to changes in cloud cover. Our findings also identify a potentially important feedback of transpiration on canopy relative humidity, $\delta^{18}O_{cv}$, and $\delta^{18}O_{lw}$, and thus on leaf-to-atmosphere CO_2 isofluxes. We believe that some of the unexplained variation in $\delta^{18}O_a$ is driven by changes in clouds given the strong responses we show here and decadal-scale changes in cloud cover and aerosols observed in many locations.

Acknowledgements

We gratefully acknowledge support from the NOAA Climate Program Office (grant number NA03OAR4310059). Data were obtained from the Atmospheric Radiation Measurement (ARM) Program sponsored by the U.S. Department of Energy, Office of Science, Office of Biological and Environmental Research, Environmental Sciences Division, under Contract No. DE-AC02-05CH11231. We also acknowledge meteorological data support provided by the Oklahoma and Kansas Mesonet Program. The US Network for Isotopes in Precipitation (http://www.uaa.alaska.edu/enri/usnip/index.cfm) contributed $\delta^{18}O$ data for our simulations and was supported in part by NSF Earth System History Program (0080952). Comments from anonymous reviewers and the associate editor improved the manuscript.

References

Ackerman, T.P., and G. Stokes (2003), The Atmospheric Radiation Measurement Program, *Physics Today, 56,* 38-45.

Affek, H.P., Krisch, M.J., and D. Yakir (2006), Effects of intraleaf variations in carbonic anhydrase activity and gas exchange on leaf $C^{18}OO$ isoflux in Zea mays, *New Phyt.*, *169(2),* 321-329.

Allison, G.B., Barnes, C.J., and M.W. Hughes, (1983), The distribution of deuterium and O-18 In dry soils. 2. Experimental, *Journal of Hydrology 64 (1-4),* 377-397.

Alton, P. North, J. Kaduk and S. Los (2005), Radiative transfer modeling of direct and diffuse sunlight in a Siberian pine forest, *J. Geophys. Res.* 110:D23209.

Amundson, R., *et al.* (1998), The isotopic composition of soil and soil-respired CO_2, *Geoderma*, *82*, 83-114.

Aranibar, J.N., Berry, J.A., Riley, W.J., *et al.* (2006), Combining meteorology, eddy fluxes, isotope measurements, and modeling to understand environmental controls of carbon isotope discrimination at the canopy scale, *Global Change Biology, 12(4),* 710-730.

Asner, G.P., *et al.* (2003), Global synthesis of leaf area index observations: implications for ecological and remote sensing studies, *Glob. Ecol. Biogeog., 12(3),* 191-205.

Baldocchi, D.D., and D.R. Bowling (2003), Modelling the discrimination of $^{13}CO_2$ above and within a temperate broad-leaved forest canopy on hourly to seasonal time scales. *Plant, Cell & Environment*, *26*, 231-244.

Barbour, M.M., Roden, J.S., Farquhar, G.D. and J.R. Ehleringer (2004), Expressing leaf water and cellulose oxygen isotope ratios as enrichment above source water reveals evidence of a Peclet effect, *Oecologia, 138(3)*, 426-435.

Barbour, M.M., *et al.* (2007), A new measurement technique reveals temporal variation in δ18O of leaf-respired CO2, *Plant, Cell & Environment*, 30(4), 456-468.

Beale, C.V., and S.P. Long (1995), Can perennial C-4 grasses attain high efficiencies of radiant energy-conversion in cool climates? *Plant, Cell and Environment,* 18**,** 641–650.

Berry, J.A., and O. Björkman (1980), Photosynthetic response and adaptation to temperature in higher plants, *Ann. Rev. Plant Phys*., *31*, 491-543.

Betts, A.K., and J.H. Ball (1998), FIFE surface climate and site-average dataset 1987-89, *Journal of the Atmospheric Sciences, 55(7),* 1091-1108.

Bonan, G.B. (1994), Comparison of two land surface process models using prescribed forcings, *Journal of Geophysical Research (Atmospheres)*, *99*, 25803-25818.

Bonan, G. (1996), A land surface model (LSM version 1.0) for ecological, hydrological, and atmospheric studies: Technical description and user's guide. TN-417+STR, NCAR, Boulder, CO.

Bonan, G.B., *et al*. (1997), Comparison of the NCAR LSM I land surface model with BOREAS aspen and jack pine tower fluxes, *Journal of Geophysical Research*, *102*, 29,065-029,076.

Bowen, G.J., and B. Wilkinson (2002), Spatial distribution of $\delta^{18}O$ in meteoric precipitation, *Geology*, *30(4)*, 315-318.

Bradford, J.B., Hicke, J.A. and W.K. Lauenroth (2005), The relative importance of light-use efficiency modifications from environmental conditions and cultivation for estimation of large-scale net primary productivity, *Remote Sensing of Environment, 96(2)*, 246-255.

Brenninkmeier, C., Kraft, K., and W. Mook (1983), Oxygen isotope fractionation between CO_2 and H_2O, *Isot. Geosci., 1*, 181– 190.

Brodersen, C.R., Vogelmann, T.C., Williams, W.E., and H.L. Gorton (2008), A new paradigm in leaf-level photosynthesis: direct and diffuse lights are not equal, *Plant, Cell and Environment, 31*, 159–164.

Buenning, N., *et al.* (*in preparation*) Modeling the response of the terrestrial biosphere and $\delta^{18}O$ of atmospheric CO_2 to flux, humidity, and isotope hydrology changes.

Campbell, J.L., Burrows, S., Gower, S.T., *et al.* (1999), *BigFoot: Characterizing Land Cover, LAI, and NPP at the Landscape Scale for EOS/MODIS Validation,* Field Manual, Version 2.1, Environmental Sciences Division, Oak Ridge National Laboratory, Pak Ridge, TN.

Cappa, C.D., Hendricks, M.B., DePaolo, D.J., and R.C. Cohen (2003), Isotopic fractionation of water during evaporation, *Journal of Geophysical Research (Atmospheres)*, *108,* D16, 4525.

Cernusak, L.A., Pate, J.S. and G.D. Farquhar (2002), Diurnal variation in the stable isotope composition of water and dry matter in fruiting Lupinus angustifolius under field conditions, *Plant Cell and Environment, 25(7)*, 893-907.

Cernusak, L.A., Farquhar, G.D., Wong, S.C., and H. Stuart-Williams (2004), Measurement and interpretation of the oxygen isotope composition of carbon dioxide respired by leaves in the dark, *Plant Physiology, 136*, 3350–3363.

Cernusak, L.A., Farquhar, G.D. and J.S. Pate (2005), Environmental and physiological controls over oxygen and carbon isotope composition of Tasmanian blue gum, Eucalyptus globulus, *Tree Physiology, 25(2)*, 129-146.

Chapin, F.S. III, Matson, P.A., and H.A. Mooney (2002), *Principles of Terrestrial Ecosystem Ecology*, Springer-Verlag, New York, 436 pp.

Choudhury, B.J. (2001), Modeling radiation- and carbon-use efficiencies of maize, sorghum, and rice, *Agricultural and Forest Meteorology,* 106, 317-330.

Ciais, P., Tans, P.P., Trolier, M., White, J.W.C. and R.J. Francey (1995), A large northern-hemisphere terrestrial CO2 sink indicated by the C-13/C-12 ratio of atmospheric CO2, *Science, 269 (5227)*, 1098-1102.

Ciais, P., *et al.* (1997a), A three-dimensional synthesis study of delta O-18 in atmospheric CO2 .1. Surface fluxes. *Journal of Geophysical Research-Atmospheres*, *102*, 5857-5872.

Ciais P, *et al.* (1997b) A three-dimensional synthesis study of delta O-18 in atmospheric CO2 .2. Simulations with the TM2 transport model. *Journal of Geophysical Research-Atmospheres, 102,* 5873-5883.

Collatz, G.J., *et al.* (1991), Physiological and environmental regulation of stomatal conductance, photosynthesis and transpiration: a model that includes a laminar boundary layer, *Agric. For. Meteorol.*, *54*, 107-136.

Collatz, G.J., *et al.* (1992), Coupled photosynthesis-stomatal conductance model for leaves of C_4 plants, *Aust. J. Plant Physiol*., *19*, 519-538.

Collatz, G.J., Berry, J.A., and J.S. Clark (1998), Effects of climate and atmospheric CO2 partial pressure on the global distribution of C-4 grasses: present, past, and future, *Oecologia, 114(4)*, 441-454, 1998.

Cooley, H.S., *et al*. (2005), Impact of agricultural practice on regional climate in a coupled land surface mesoscale model, *J Geophys Res-Atmos*, *110*.

Cousins, A.B., Badger, M.R., and S. von Caemmerer (2006), A transgenic approach to understanding the influence of carbonic anhydrase on $C^{18}OO$ discrimination during photosynthesis, *Plant Physiology, 142*, 662–672.

Craig, H., and L. Gordon (1965), In *Proc. Conf. Stable Isotopes in Oceanographic Studies and Paleotemp.* 9-130 (Laboratory of Geology and Nuclear Science, Pisa).

Cuntz, M., *et al* (2003a), A comprehensive global three-dimensional model of delta O-18 in atmospheric CO2: 1. Validation of surface processes, *J. Geophys Res-Atmos, 108*.

Cuntz, M., *et al* (2003b), A comprehensive global three-dimensional model of delta O-18 in atmospheric CO2: 2. Mapping the atmospheric signal, *J. Geophys Res-Atmos, 108*.

Dai, A., Trenberth, K.E., and T.R. Karl (1999), Effects of clouds, soil moisture, precipitation, and water vapor on diurnal temperature range, *J. Climate, 12*, 2451-2473.

Daughtry, C.S.T., Gallo, K.P., Goward, S.N., Prince, S.D. and W.P. Kustas (1992), Spectral estimates of absorbed radiation and phytomass production in corn and soybean canopies, *Remote Sensing of Environment, 39(2)*, 141-152.

de Pury, D.G.G., and G.D. Farquhar (1997), Simple scaling of photosynthesis from leaves to canopies, *Plant, Cell and Environment, 20*, 537-557.

Dickinson, R. (1983), Land surface processes and climate-surface albedos and energy balance, *Adv. Geophys.*, *25*, 305-353.

Dong, X., Xi, B., and P. Minnis (2006), Observational evidence of changes in water vapor, clouds, and radiation at the ARM SGP site, *Geophys. Res. Ltrs.*, *33*, L19818.

Dongmann, G., Nürnberg, H.W., Förstel, H., and K. Wagener (1974), On the enrichment of $H_2^{18}O$ in the leaves of transpiring plants, *Radiation and Enviromental Biophysics, 11*, 41–52.

Ehleringer, J.R., Cerling, T.E. and B.R. Helliker (1997), C-4 photosynthesis, atmospheric CO2 and climate, *Oecologia, 112(3)*, 285-299.

Evans JR, and F. Loreto (2000), Acquisition and diffusion of CO_2 in higher plant leaves, In: Leegood RC, Sharkey TD, von Caemmerer S. eds, *Photosynthesis: physiology and metabolism*. Dordrecht: Kluwer Academic Publishers, 321–351.

Farquhar, G.D., von Caemmerer, S. and J.A. Berry (1980), A biochemical-model of photosynthetic CO2 assimilation in leaves of C-3 species, *Planta, 149(1)*, 78-90.

Farquhar, G.D., and T.D. Sharkey (1982), Stomatal conductance and photosynthesis, *Ann. Rev. Plant Physiol. Plant Molecular Bio., 33,* 317-345.

Farquhar, G.D., J.R. Ehleringer, and K.T. Hubick, Carbon Isotope Discrimination and Photosynthesis, Annual Review of Plant Physiology and Plant Molecular Biology, 40, 503-537, 1989.

Farquhar GD, Hubick KT, Condon AG, Richards RA (1989) Carbon isotope fractionation and plant water-use efficiency. In PW Rundel, JR Ehleringer, KA Nagy, eds, *Stable isotopes in ecological research*. Springer-Verlag, New York, pp 21-40.

Farquhar, G. D., and J. Lloyd. (1993), Carbon and oxygen isotope effects in the exchange of carbon dioxide between plants and the atmosphere, pages 47–70 in J. R. Ehleringer, A. E. Hall, and G. D. Farquhar, editors. *Stable isotopes, and plant carbon–water relations*. Academic Press, New York, New York, USA.

Farquhar, G.D., *et al.* (1993), Vegetation effects on the isotope composition of oxygen in atmospheric CO_2, *Nature 363*, 439-443.

Farquhar, G.D., and L.A. Cernusak (2005), On the isotopic composition of leaf water in the non-steady state, *Functional Plant Biology, 32(4)*, 293-303.

Field, C.B., Behrenfeld, M.J., Randerson, J.T. *et al.* (1998), Primary production of the biosphere: integrating terrestrial and oceanic components, *Science*, *281,* 237–240.

Fischer, D.T., Still, C.J., and A.P. Williams (in press), Significance of summer overcast and fog to drought stress and ecological functioning of coastal California endemic species, *J. Biogeog*.

Flanagan, L.B., *et al.* (1991), Comparison of modeled and observed environmental influences on the stable oxygen and hydrogen isotope composition of leaf water in *Phaseolus-vulgaris, Plant Physiology, 96*, 588-596.

Flanagan, L.B., *et al.* (1994), Effect of changes in leaf water oxygen isotopic composition on discrimination against (COO)-O-18-O-16 during photosynthetic gas exchange. *Australian Journal of Plant Physiology, V21*, 221-234.

Flanagan, L.B. (2005), Ecosystem CO_2 exchange and variation in the $\delta^{18}O$ of atmospheric CO_2, In *Stable Isotopes and Biosphere-Atmosphere Interactions* (Eds. Flanagan, L.B., Ehleringer, J.R. & D.E. Pataki). Elsevier-Academic Press, Physiological Ecology Series, San Diego, CA

Förstel H (1978), The enrichment of ^{18}O in leaf water under natural conditions, *Radiat Environ. Biophys. 15*, 323–344.

Francey, R.J., *et al.* (1995), Changes in oceanic and terrestrial carbon uptake since 1982, *Nature, 373 (6512)*, 326-330.

Francey, R.J., and P.P. Tans (1987), Latitudinal variation in oxygen-18 of atmospheric CO_2, *Nature, 327*, 495-497.

Freedman, J.M., Fitzjarrald, D.R., Moore, K.E., and R.K. Sakai (2001), Boundary layer clouds and vegetation-atmosphere feedbacks, *Journal of Climate, 14(2)*, 180-197.

Friedli, H., Siegenthaler, U., Rauber, D., and H. Oeschger (1987), Measurements of concentration, 13C/12C and 18O/16O ratios of tropospheric carbon dioxide over Switzerland, *Tellus, 39B,* 80-88.

Fung, I., *et al.* (1997), Carbon 13 exchanges between the atmosphere and biosphere, *Global Biogeochemical Cycles, 11(4)*, 507-533.

Gillon, J.S., and D. Yakir (2000), Naturally low carbonic anhydrase activity in C-4 and C-3 plants limits discrimination against (COO)-O-18 during photosynthesis. *Plant Cell and Environment, 23*, 903-915.

Gillon, J.S., and D. Yakir (2001), Influence of carbonic anhydrase activity in terrestrial vegetation on the O-18 content of atmospheric CO2. *Science*, *291*, 2584-2587.

Gower, S.T., Kucharik, C., and J. Norman (1999), Direct and indirect estimation of leaf area index, f(APAR), and net primary production of terrestrial ecosystems, *Remote Sensing of the Environment, 70,* 29-51.

Graham, E.A., Mulkey, S.S., Kitajima, K., Phillips, N.G., and S.J. Wright (2003), Cloud cover limits net CO2 uptake and growth of a rainforest tree during tropical rainy seasons, *Proceedings of the National Academy of Sciences of the United States of America, 100(2)*, 572-576.

Griffis, T.J., Lee, X., Baker, J.M., Sargent, S.D., and J.Y. King (2005), Feasibility of quantifying ecosystem–atmosphere C18O16O exchange using laser spectroscopy and the flux-gradient method, *Agricultural and Forest Meteorology*, *135(1-4),* 44-60.

Griffis, T.J., Sargent, S.D., Baker, J.M., Lee, X., Tanner, B.D., Greene, J., Swiatek, E., and K. Billmark (2008), Direct measurement of biosphere-atmosphere isotopic CO_2 exchange using the eddy covariance technique, *Journal of Geophysical Research*, *113*, D08304, doi:10.1029/2007JD009297.

Gu, L.H., Shugart, H.H., Fuentes, J.D., Black, T.A. and S.R. Shewchuk (1999), Micrometeorology, biophysical exchanges and NEE decomposition in a two-story boreal forest - development and test of an integrated model, *Agricultural and Forest Meteorology, 94(2)*, 123-148.

Gu, L., Fuentes, J.D., Shugart, H.H., *et al.* (2001), Cloud modulation of surface solar irradiance at a pasture site in southern Brazil, *Agricultural and Forest Meteorology*, *106,* 117-129.

Gu, L., Baldocchi, D.D., Verma, S.B., *et al.* (2002), Superiority of diffuse radiation for terrestrial ecosystem productivity, *Journal of Geophysical Research, 107,* D6, 4050.

Gu, L., Baldocchi, D.D., Wofsy, S.C., *et al.* (2003), Response of a deciduous forest to the Mount Pinatubo eruption: enhanced photosynthesis, *Science*, *299,* 2035-2038.

Harwood, K.G., Gillon, J.S., Griffiths, H., and M.S.J. Broadmeadow (1998), Diurnal variation in $\Delta^{13}CO_2$, $\Delta C^{18}O^{16}O$ and evaporative site enrichment of $\delta H_2{}^{18}O$ in *Piper aduncum* under field conditions in Trinidad, *Plant, Cell and Environment, 21*, 269-283.

Helliker, B.R., and J.R. Ehleringer (2000), Establishing a grassland signature in veins: O-18 in the leaf water of C-3 and C-4 grasses. *Proceedings of the National Academy of Sciences of the United States of America, 97*, 7894-7898.

Helliker, B.R., *et al.* (2002) A rapid and precise method for sampling and determining the oxygen isotope ratio of atmospheric water vapor. *Rapid Comm. Mass Spectrometry, 16*, 929-932.

Hollinger, D.Y., Kelliher, F.M., Byers, J.N., *et al.* (1994), Carbon dioxide exchange between an undisturbed old-growth temperate forest and the atmosphere, *Ecology, 75(1),* 134-150.

Hollinger, D.Y., Kelliher, F.M., Schulze, E.D., *et al.* (1998), Forest-atmosphere carbon dioxide exchange in eastern Siberia, *Agricultural and Forest Meteorology, 90,* 291-306.

Horita, J., and D.J. Wesolowski (1994), Liquid-vapor fractionation of oxygen and hydrogen isotopes of water from the freezing to the critical temperature, *Geochim. Cosmochim. Acta*, *58(16)*, 3425-3437.

Ishizawa, M., Nakazawa, T., and K. Higuchi (2002), A multi-box model study of the role of the biospheric metabolism in the recent decline of $\delta^{18}O$ in atmospheric CO_2, *Tellus*, *54B,* 307-324.

Johnson, D.M., and W.K. Smith (2006), Low clouds and cloud immersion enhance photosynthesis in underrstory species of a southern Appalachian spruce-fir forest (USA), *Am. J. Bot.*, *93(11),* 1625-1632.

Johnson, D.M., and W.K. Smith (2008), Cloud immersion alters microclimate, photosynthesis and water relations in *Rhododendron catawbiense* and *Abies fraseri* seedlings in the southern Appalachian Mountains, USA, *Tree Phys*., 28, 385–392.

Jones, H.G. (1992), *Plants and microclimate: A quantitative approach to environmental plant physiology*. Cambridge University Press, Cambridge, UK, 428 pp.

Knohl, A., and D.D. Baldocchi (2008), Effects of diffuse radiation on canopy gas exchange processes in a forest ecosystem, *J. Geophys. Res*., 113, G02023, doi:10.1029/2007JG000663.

Lai, C.-T., Ehleringer, J.R., Bond, B.J., and U.K.T. Paw (2005), Contributions of evaporation, isotopic non-steady state transpiration, and atmospheric mixing on the $\delta^{18}O$ of water vapor in Pacific Northwest coniferous forests, *Plant, Cell and Environment, 29,* 77-94.

Lai, C.-T., Riley, W.J, Owensby, C., Ham, J., and J.R. Ehleringer (2006), Seasonal and interannual variations of carbon and oxygen isotopes of respired CO2 in a tallgrass prairie: Measurements and modeling results from 3 years with contrasting water availability, *J. Geophysical Research, 111,* D08S06, doi:10.1029/2005JD006436.

Larcher, W. (2003), *Physiological Plant Ecology*, 4th edition, Springer, Berlin, 513 pp.

Lee, X., Smith, R., Williams, J. (2006), Water vapour $^{18}O/^{16}O$ isotope ratio in surface air in New England, USA, *Tellus 58B,* 293-304.

Leuning, R., Kelliher, F.M., de Pury, D.G.G., Schulze, E.-D. (1995), Leaf nitrogen, photosynthesis, conductance and transpiration: scaling from leaves to canopy, *Plant, Cell and Environment 18*, 1183-1200.

Liepert, B.G. (2002), Observed reductions of surface solar radiation at sites in the United States and worldwide from 1961 to 1990, *Geophysical Research Letters, 29(10).*

Liepert, B.G., Feichter, J., Lohmann, U., and E. Roeckner (2004), Can aerosols spin down the water cycle in a warmer and moister world?, *Geophysical Research Letters, 31(6).*

Lobell, D.B., J.A. Hicke, G.P. Asner, C.B. Field, C.J. Tucker, and S.O. Los, Satellite estimates of productivity and light use efficiency in United States agriculture, 1982-98, Global Change Biology, 8 (8), 722-735, 2002.

Long, S.P. (1999), Environmental responses, in *C4 Plant Biology*, edited by R.F. Sage and R.K. Monson, pp. 215-249, Academic Press, New York.

Long, S.P., Zhu, X-G., Naidu, S.L., and D.R. Ort (2006), Can improvement in photosynthesis increase crop yields?, *Plant, Cell and Environment, 29,* 315-330.

Lynch J.A., Grimm J.W., and V.C. Bowersox (1995), Trends in precipitation chemistry in the United States: a national perspective, 1980-1992, *Atmospheric Environment, 29(11),* 1231-46.

McDowell, N., *et al.* (2008), Understanding the stable isotope composition of biosphere-atmosphere CO_2 exchange, *Eos*, 89 (10), 94-95.

Miller, J.B., Yakir, D., White, J.W.C., and P.P. Tans (1999), Measurement of O-18/O-16 in the soil-atmosphere CO_2 flux, *Global Biogeochemical Cycles, 13,* 761-774.

Min, Q. (2005), Impacts of aerosols and clouds on forest-atmosphere carbon exchange, *J. Geophys. Res.*, *110,* D06203.

Min, Q. and S. Wang (2008), Clouds modulate terrestrial carbon uptake in a midlatitude hardwood forest, *Geophys. Res. Ltrs., 35,* L02406.

Morison, J.I.L., *et al.* (2000), Very high productivity of the C_4 aquatic grass *Echinochloa polystachya* in the Amazon floodplain confirmed by net ecosystem CO_2 flux measurements, *Oecologia*, *125,* 400-411.

Niyogi D., *et al.* (2004), Direct observations of the effects of aerosol loading on net ecosystem CO_2 exchanges over different landscapes, *Geophys. Res. Ltrs*., *31,* L20506.

Noone, D., C. Still, W. Riley, L. Welp and J. Randerson (2004), Isotopic diagnosis of processes governing interannual variability of CO18O fluxes in the tropics, *Eos Trans. AGU, 85 Jt. Assem. Suppl.*, Abstract B41B-02.

Norman, J.M., and T.J. Arkebauer (1991), Predicting canopy light-use efficiency from leaf characteristics, in *Modeling Plant and Soil Systems*, *Agron. Monogr.*, vol. 31, pp. 125-143, Am. Soc. Of Agron., Madison, WI.

Ogée, J., Peylin, P., Cuntz, M., *et al.* (2004), Partitioning net ecosystem carbon exchange into net assimilation and respiration with canopy-scale isotopic measurements: an error propagation analysis with 13CO2 and CO18O data, *Glob. Biogeochem. Cycles, 18 (2),* GB2019.

Oliveira, P.H.F., *et al.* (2007), The effects of biomass burning aerosols and clouds on the CO_2 flux in Amazonia, *Tellus, 59B,* 338-349.

Ometto, J.P.H., Flanagan, L.B., Martinelli, L.A. and J.R. Ehleringer (2005), Oxygen isotope ratios of waters and respired CO2 in Amazonian forest and pasture ecosystems, *Ecological Applications, 15(1)*, 58-70.

Pataki, D., *et al.* (2003), The application and interpretation of Keeling plots in terrestrial carbon cycle research, *Glob. Biogeochem. Cycles, 17(1)* 1022.

Peylin P, *et al.* (1999), A 3-dimensional study of delta O-18 in atmospheric CO2: contribution of different land ecosystems. *Tellus Series B-Chemical and Physical Meteorology, 51*, 642-667.

Piedade, M.T.F., Junk, W.J., and S.P. Long (1991), The productivity of the C_4 grass *Echinochloa polystachya* on the Amazon floodplain, *Ecology*, *72(4),* 1456-1463.

Randerson, J.T., *et al.*. (2002a), The ^{13}C discrimination of arctic and boreal biome net CO_2 exchange inferred from remote atmospheric measurements and a biosphere-atmosphere model, *Global Biogeochemical Cycles, 16(3),* 1028.

Randerson, J.T., *et al*. (2002b), A possible global covariance between terrestrial gross primary production and ^{13}C discrimination: Consequences for the atmospheric ^{13}C budget and its response to ENSO, *Global Biogeochemical Cycles*, *16(4),* 1136.

Rayner, P.J., Enting, I.G., Francey, R.J. and R. Langenfelds (1999), Reconstructing the recent carbon cycle from atmospheric CO2, delta C-13 and O-2/N-2 observations, *Tellus Series B-Chemical and Physical Meteorology, 51(2)*, 213-232.

Rayner, P.J., Law, R.M., Allison, C.E., Francey, R.J., Trudinger, C.M. and C. Pickett-Heaps (2008), Interannual variability of the global carbon cycle (1992–2005) inferred by inversion of atmospheric CO_2 and $\delta^{13}CO_2$ measurements, *Global Biogeochemical Cycles 22,* GB3008, doi:10.1029/2007GB003068.

Riley, W.J., *et al.* (2002), A mechanistic model of $H_2{}^{18}O$ and $C^{18}OO$ fluxes between ecosystems and the atmosphere: Model description and sensitivity analyses, *Global Biogeochemical Cycles*, *16*, 1095-1109.

Riley, W.J., *et al*. (2003), ^{18}O composition of CO_2 and H_2O ecosystem pools and fluxes in a tallgrass prairie: Simulations and comparisons to measurements, *Glob Change Biology*, *9*, 1567-1581.

Riley, W.J. (2005), A modeling study of the impact of the delta O-18 value of near-surface soil water on the delta O-18 value of the soil-surface CO2 flux, *Geochimica Et Cosmochimica Acta, 69(8),* 1939-1946.

Rocha, A. V., Su, H.B., Vogel, C., Schmid, H.P. and P. S. Curtis (2004), Photosynthetic and water use efficiency responses to diffuse radiation by an aspen-dominated northern hardwood forest, *For. Sci., 50(6),* 793–801.

Roderick, M.L. (1999), Estimating the diffuse component from daily and monthly measurements of global radiation, *Agricultural and Forest Meteorology, 95(3)*, 169-185.

Roderick, M.L., Farquhar, G.D., Berry, S.L., and I.R. Noble (2001) On the direct effect of clouds and atmospheric particles on the productivity and structure of vegetation, *Oecologia, 129(1)*, 21-30.

Roderick, M.L. (2006), The ever-flickering light, *Trends in Ecology & Evolution, 21(1)*, 3-5

Ruimy, A., *et al.* (1995), CO_2 fluxes over plant canopies and solar radiation: a review, *Advances in Ecological Research*, *26,* 1-68.

Ruimy, A., Kergoat, L., and A. Bondeau (1999), Comparing global models of terrestrial net primary productivity (NPP): Analysis of differences in light absorption and light-use efficiency, *Global Change Biology, 5,* 56-64.

Sage, R.F., Wedin, D.A. and M. Li (1999), The biogeography of C_4 photosynthesis: patterns and controlling factors, in *C4 Plant Biology*, edited by R.F. Sage and R.K. Monson, pp. 313-373, Academic Press, New York.

Scholze, M., Kaplan, J.O., Knorr, W. and M. Heimann (2003), Climate and interannual variability of the biosphere-atmosphere $^{13}CO_2$ flux, *Geophys. Res. Lett., 30(2),* 1097, doi:10.1029/2002GL015631.

Schwarz, A.G., and R.E. Redmann (1988), C4 grasses from the boreal forest region of northwestern Canada, *Can. J. Bot., 66,* 2424-2430.

Seibt, U., Wingate, L., Berry, J.A., and J. Lloyd (2006), Non-steady state effects in diurnal O-18 discrimination by *Picea sitchensis* branches in the field, *Plant Cell and Environment, 29(5*), 928-939.

Sellers, P.J. (1985), Canopy reflectance, photosynthesis and transpiration, *International Journal of Remote Sensing, 6,* 1335-1372.

Sellers, P.J., Randall, D.A., Collatz, G.J. *et al.* (1996), A revised land surface parameterization (SiB2 for atmospheric GCMs .1. Model formulation, *J. Climate*, *9*, 676-705.

Stanhill, G., and S. Cohen, Solar radiation changes in the United States during the Twentieth Century: Evidence from sunshine measurements, *Journal of Climate, 18 (10)*, 1503-1512, 2005.

Stern, L.A., Amundson, R., and W.T. Baisden (1999), Processes controlling the oxygen isotope ratio of soil CO_2: Analytic and numerical modeling, *Geochim. Cosmochim. Acta, 63,* 799-814.

Stern, L.A., Amundson, R., and W.T. Baisden (2001), Influence of soils on oxygen isotope ratio of atmospheric CO_2, *Global Biogeochemical Cycles, 15*, 753-759.

Still, C.J., Berry, J.A., Collatz, G.J., and R.S. DeFries (2003), The global distribution of C_3 and C_4 vegetation: carbon cycle implications, *Glob. Biogeochem. Cycles, 17(1),* 1006.

Still, C.J., *et al.* (2005), Simulation of ecosystem $C^{18}OO$ isotope fluxes in a tallgrass prairie: biological and physical controls. In *Stable Isotopes and Biosphere-Atmosphere Interactions* (Eds. Flanagan, L.B., Ehleringer, J.R. & D.E. Pataki). Elsevier-Academic Press, Physiological Ecology Series.

Suyker, A.E., and S.B. Verma (2001), Year-round observations of the net ecosystem exchange of carbon dioxide in a native tallgrass prairie, *Global Change Biology 7,* 279-289.

Tans, P.P. (1998), Oxygen isotopic equilibrium between carbon dioxide and water in soils, *Tellus Series B-Chemical and Physical Meteorology, 50*, 163-178.

Turner, D.P., Urbanski, S., Bremer, D., *et al*. (2003) A cross-biome comparison of daily light use efficiency for gross primary production. *Global Change Biology,* 9, 383-395.

Urban, O., *et al.* (2007), Ecophysiological controls over the net ecosystem exchange of mountain spruce stand. Comparison of the response in direct vs. diffuse solar radiation. *Global Change Biology, 13*, 157-168.

Vachon, R., White, J. W., Gutmann, E., and J.M. Welker (2007), Amount-weighted annual isotopic (^{18}O) values are affected by the seasonality of precipitation: a sensitivity study, *Geophys. Res. Letts. 34*, L 21707.

von Caemmerer, S., and R.T. Furbank (2003), The C_4 pathway: an efficient CO_2 pump. *Photosynthesis Research, 77*, 191–207.

Wang, Y.P., and R. Leuning (1998), A two-leaf model for canopy conductance, photosynthesis and partitioning of available energy I: Model description and comparison with a multi-layered model, *Agricultural and Forest Meteorology, 91(1-2)*, 89-111.

Wang, X.J. and J.R. Key (2003), Recent trends in arctic surface, cloud, and radiation properties from space, *Science, 299(5613),* 1725-1728.

Welker, J. (2000), Isotopic ($\delta^{18}O$) characteristics of weekly precipitation collected across the USA: an initial analysis with application to water source studies. *Hydrol. Proc., 14,* 1449-1464.

Welp, L.R., Randerson, J.T., and H.P. Liu (2006), Seasonal exchange of CO_2 and $\delta^{18}O$-CO_2 varies with postfire succession in boreal forest ecosystems. *J. Geophys. Res.*, *111*, G03007.

White, J.W.C., and S.D. Gedzelman (1984), The isotope composition of atmospheric water vapor and the concurrent meteorological conditions, *J. Geophys. Res.*, *89*, 4937-4939.

Wielicki, B.A., *et al.* (2002), Evidence for large decadal variability in the tropical mean radiative energy budget, *Science, 295(5556)*, 841-844.

Wild, M., *et al*. (2005), From dimming to brightening: Decadal changes in surface solar radiation, *Science*, *308,* 847-850.

Wild, M., Ohmura, A., Makowski, K. (2007), Impact of global dimming and brightening on global warming, *Geophys. Res. Ltrs., 34*, L04702.

Williams, A.P., Still, C.J., Fischer, D.T., and S.W. Leavitt (2008), The influence of summertime fog and overcast clouds on the growth of a coastal Californian pine: a tree-ring study. *Oecologia* doi: 10.1007/s00442-008-1025-y.

Woodrow, I.E., and J.A. Berry (1988), Enzymatic regulation of photosynthetic CO2 fixation in C-3 plants, *Annual Review of Plant Physiology and Plant Molecular Biology*, *39*, 533-594.

Yakir, D., and Y.Israeli (1995), Reduced solar irradiance effects on net primary productivity (NPP) and the $\delta^{13}C$ and $\delta^{18}O$ values in plantations of *Musa* sp., *Musaceae*, *Geochim. Cosmochim. Acta, 59(10),* 2149-2151.

Yakir, D., and L.D.L. Sternberg (2000), The use of stable isotopes to study ecosystem gas exchange, *Oecologia, 123(3)*, 297-311.

Zundel, G., Miekeley, W., Grisi, B.M. and H. Forstel (1978), (H2o)-O-18 enrichment in leaf water of tropic trees - comparison of species from tropical rain-forest and semi-arid region in Brazil, *Radiation and Environmental Biophysics, 15(2)*, 203-212

Figure Captions

Figure 1. (a) The observed percent cover of thick (opaque) and thin clouds at the ARM Central Facility during daylight hours from DOY 193-204 (July 11-22, 2004). (b) Observed direct and diffuse PAR irradiance (μmol ‰ m^{-2} s^{-1} - using conversion factors of 4.6 μmol photons/J and 4.2 μmol photons /J for direct and diffuse radiation – Larcher 2003) on consecutive summer days (DOY 193-204) with contrasting cloud cover.

Figure 2. Observed background relative humidity and incident diffuse PAR fraction (R_D/R_S).

Figure 3. Observed daytime thick cloud cover fraction and incident diffuse PAR fraction (R_D/R_S) over the study period (DOY 193-204). Early morning and late afternoon values were screened to minimize the impact of low solar angles (< 15º) on R_D/R_S.

Figure 4. (a) Modeled broadleaf deciduous tree canopy photosynthesis per unit ground area (μmol m^{-2} s^{-1}) during DOY 193-204. (b) Modeled tree canopy photosynthesis (μmol m^{-2} s^{-1}) plotted against the thick cloud cover percentage for daylight hours from DOY 193-204.

Figure 5. Modeled C_4 grass canopy photosynthesis (μmol m^{-2} s^{-1}) during DOY 193-204.

Figure 6. (a) Modeled gross canopy LUE (mol CO_2 mol^{-1} APAR) in the broadleaf deciduous tree canopy plotted against observed R_D/R_S during daylight hours (solar angles > 15º). (b) Modeled C_4 grass canopy gross canopy LUE (mol CO_2 mol^{-1} APAR) plotted against observed R_D/R_S during daylight hours.

Figure 7. (a) $\delta^{18}O$ (‰, relative to V-SMOW) of leaf water ($\delta^{18}O_{lw}$) for sun and shade leaves, and stem source water ($\delta^{18}O_{xy}$) and canopy vapor ($\delta^{18}O_{cv}$) in the broadleaf deciduous forest canopy simulation. (b) The same quantities plotted for the C_4 grass canopy simulation.

Figure 8. (a) Modeled photosynthetic isofluxes (μmol ‰ m^{-2} s^{-1}), $^{18}F_{al}$ and $^{18}F_{la}$, and their sum ($A_{net}{}^{18}\Delta$) for the broadleaf tree canopy. (b) The same quantities plotted for the C_4 grass canopy.

Figure 9. Modeled daytime net photosynthetic isofluxes ($A_{net}{}^{18}\Delta$ μmol ‰ m^{-2} s^{-1}) plotted against the observed daytime incident PAR for the C_4 grass canopy simulation.

Figure 10. Modeled net photosynthetic isofluxes (μmol ‰ m^{-2} s^{-1}), $^{18}F_{al}$ and $^{18}F_{la}$, and their sum for the low LAI (3.5) broadleaf tree canopy simulation.

Variable	Description
$\delta^{18}O_a$	Background atmosphere $\delta^{18}O$-CO_2 (V-PDB-CO_2)
R_D/R_S	Diffuse fraction, the ratio of diffuse irradiance to total (global) irradiance or of diffuse PAR to total PAR
PAR	Photosynthetically Active Radiation (400-700 nm).
LAI	Leaf Area Index (m^2/m^2)
$^{18}\Delta$	Discrimination against $CO^{18}O$ during photosynthesis
ε_d	Kinetic fractionation during molecular diffusion of $CO^{18}O$
$\delta^{18}O_c$	$\delta^{18}O$ value of CO_2 in equilibrium with H_2O in leaves
Ca, Ci, Cc	CO_2 concentrations in the atmosphere, stomatal pore, and in chloroplasts
F_{al}	Gross CO_2 flux from atmosphere to leaf
F_{la}	Gross CO_2 flux from leaf to atmosphere
A_{net}	Net leaf photosynthesis including leaf respiration (F_{al}-F_{la})
$^{18}F_{al}$	Atmosphere-to-leaf isoflux ($\delta^{18}O$ in CO_2)
$^{18}F_{la}$	Leaf-to-atmosphere isoflux ($\delta^{18}O$ in CO_2)
$A_{net}{}^{18}\Delta$	Net photosynthetic isoflux
$\delta^{18}O_{lw}$	$\delta^{18}O$ value of leaf water (V-SMOW)
$\delta^{18}O_{xy}$	$\delta^{18}O$ composition of source water in xylem (V-SMOW)
$\delta^{18}O_{sw}$	$\delta^{18}O$ composition of soil water (V-SMOW)
$\delta^{18}O_{cv}$	$\delta^{18}O$ composition of in-canopy water vapor (V-SMOW)
$\delta^{18}O_v$	$\delta^{18}O$ composition of background, above-canopy water vapor (V-SMOW)

Table 1. Nomenclature used in paper, where $\delta = \left(\frac{R_{sam}}{R_{std}} - 1\right)$ and R_{sam} and R_{std} are the ratios of $^{18}O/^{16}O$ in a sample or standard, respectively. $\delta^{18}O$-CO_2 values are reported relative to the V-PDB-CO_2 measurement scale, and $\delta^{18}O$-H_2O values are reported relative to the V-SMOW measurement scale.

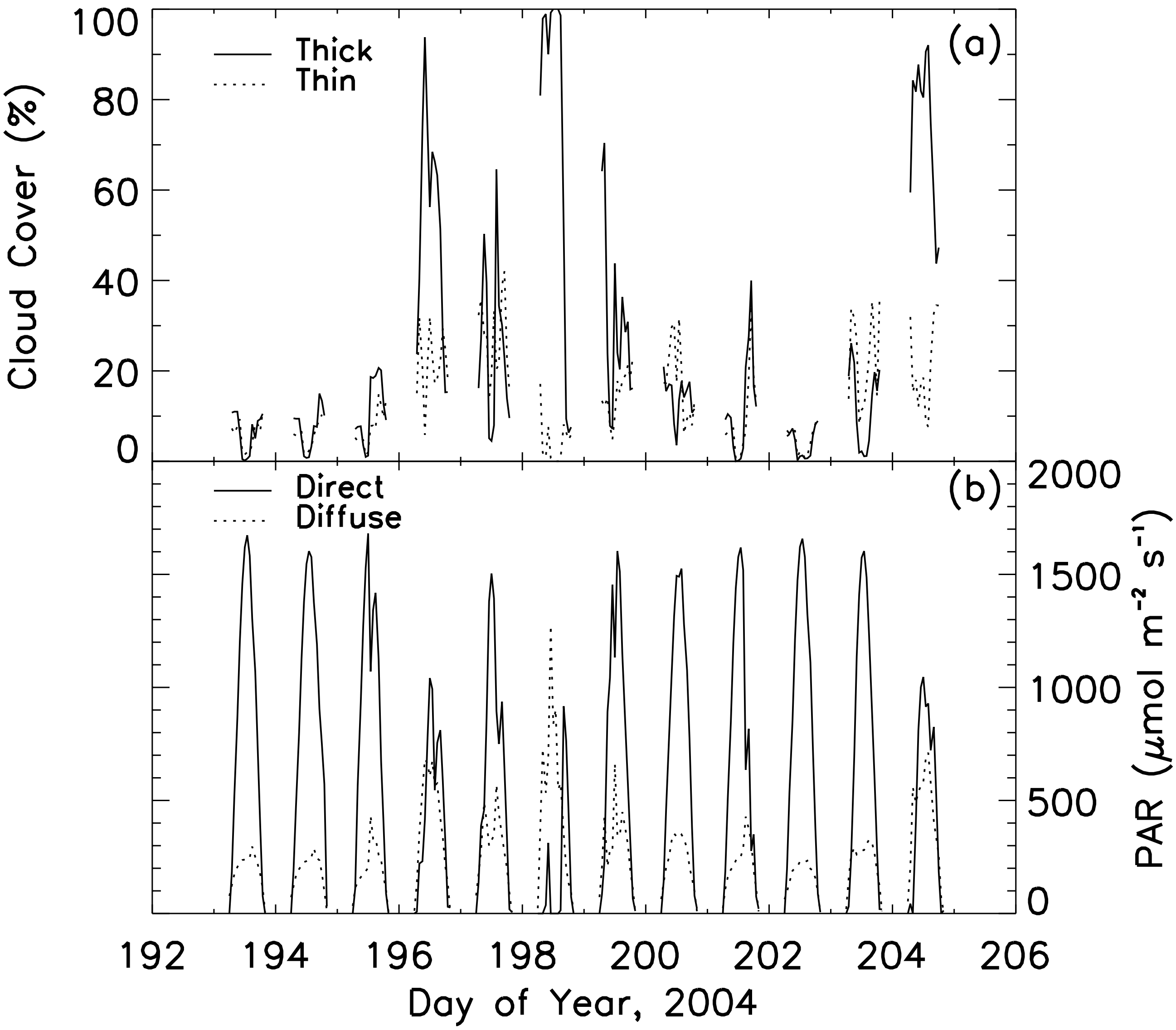

Thick
Thin
(a)
Cloud Cover (%)
100
80
60
40
20
0
Direct
Diffuse
(b)
PAR (μmol m⁻² s⁻¹)
2000
1500
1000
500
0
192
194
196
198
200
202
204
206
Day of Year, 2004

Figure 1

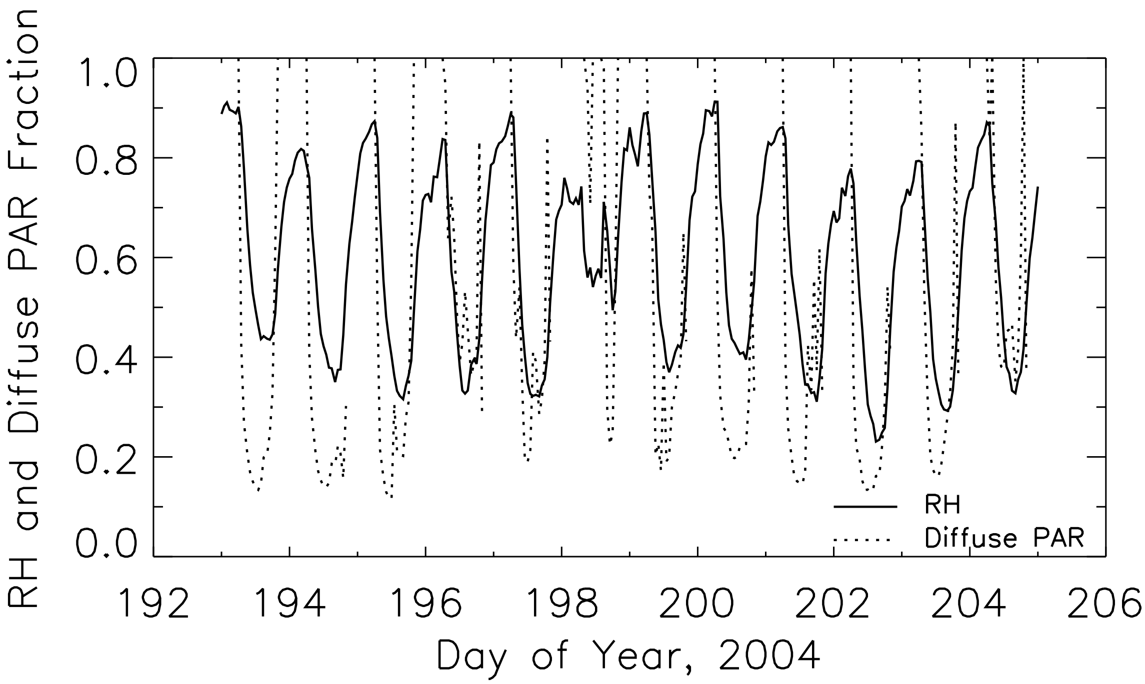

RH and Diffuse PAR Fraction
1.0
0.8
0.6
0.4
0.2
0.0
192
194
196
198
200
202
204
206
Day of Year, 2004
RH
Diffuse PAR

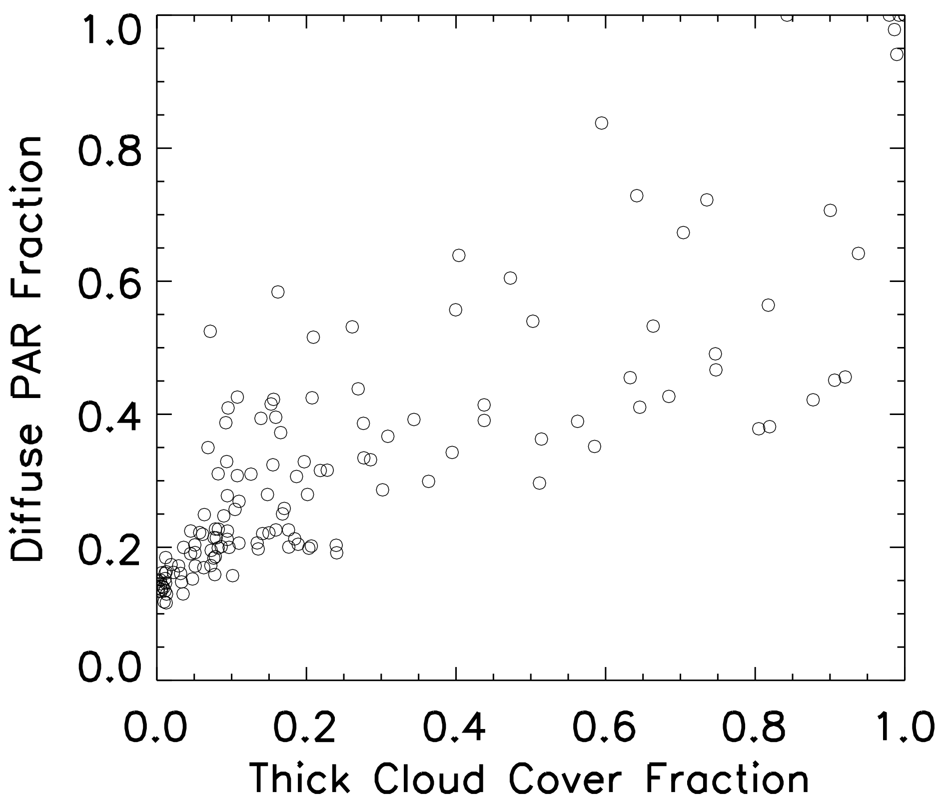
1.0
0.8
0.6
0.4
0.2
0.0
Diffuse PAR Fraction
0.0
0.2
0.4
0.6
0.8
1.0
Thick Cloud Cover Fraction

Figure 3

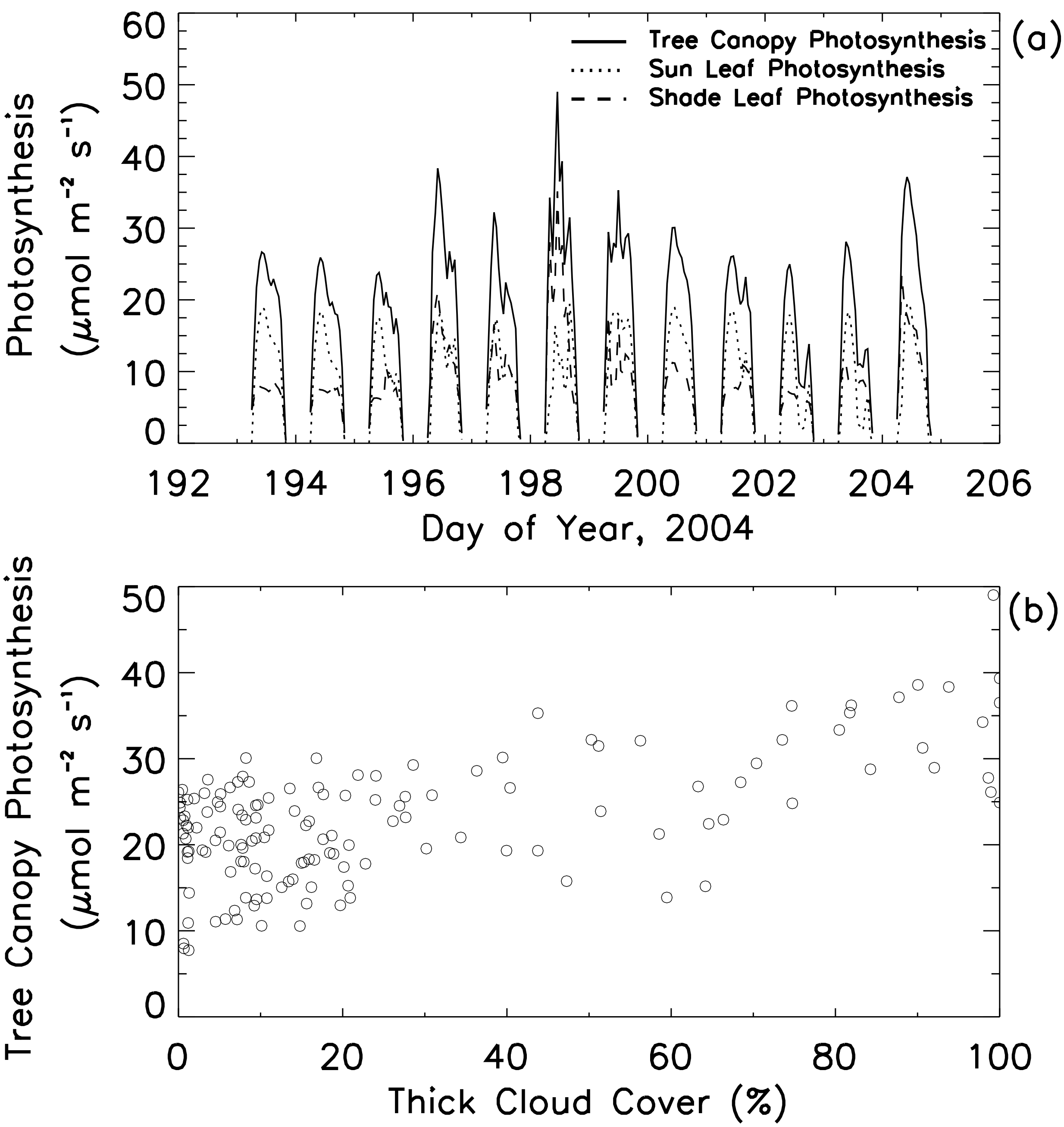
Tree Canopy Photosynthesis
Sun Leaf Photosynthesis
Shade Leaf Photosynthesis
(a)
Photosynthesis
(μmol m⁻² s⁻¹)
0
10
20
30
40
50
60
192
194
196
198
200
202
204
206
Day of Year, 2004
(b)
Tree Canopy Photosynthesis
(μmol m⁻² s⁻¹)
0
10
20
30
40
50
0
20
40
60
80
100
Thick Cloud Cover (%)

Figure 4

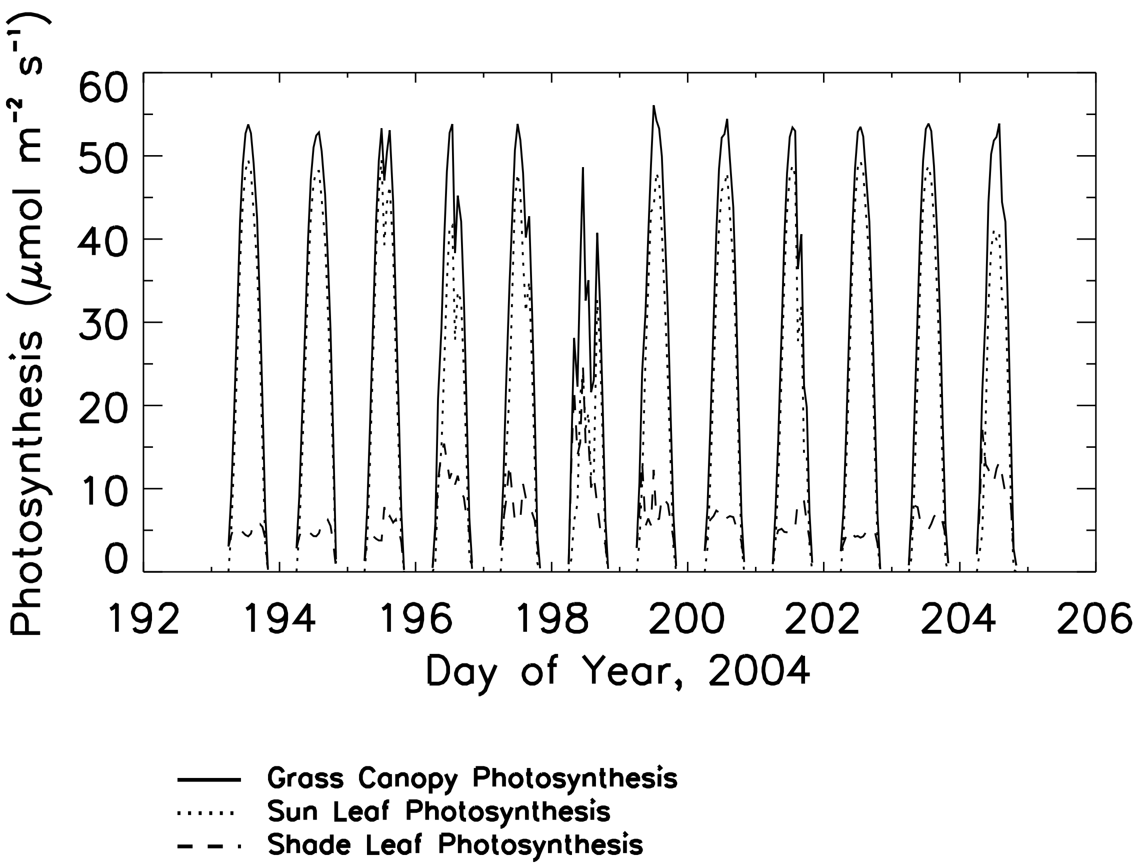
Photosynthesis (μmol m^{-2} s^{-1})
60
50
40
30
20
10
0
192
194
196
198
200
202
204
206
Day of Year, 2004
Grass Canopy Photosynthesis
Sun Leaf Photosynthesis
Shade Leaf Photosynthesis

Figure 5

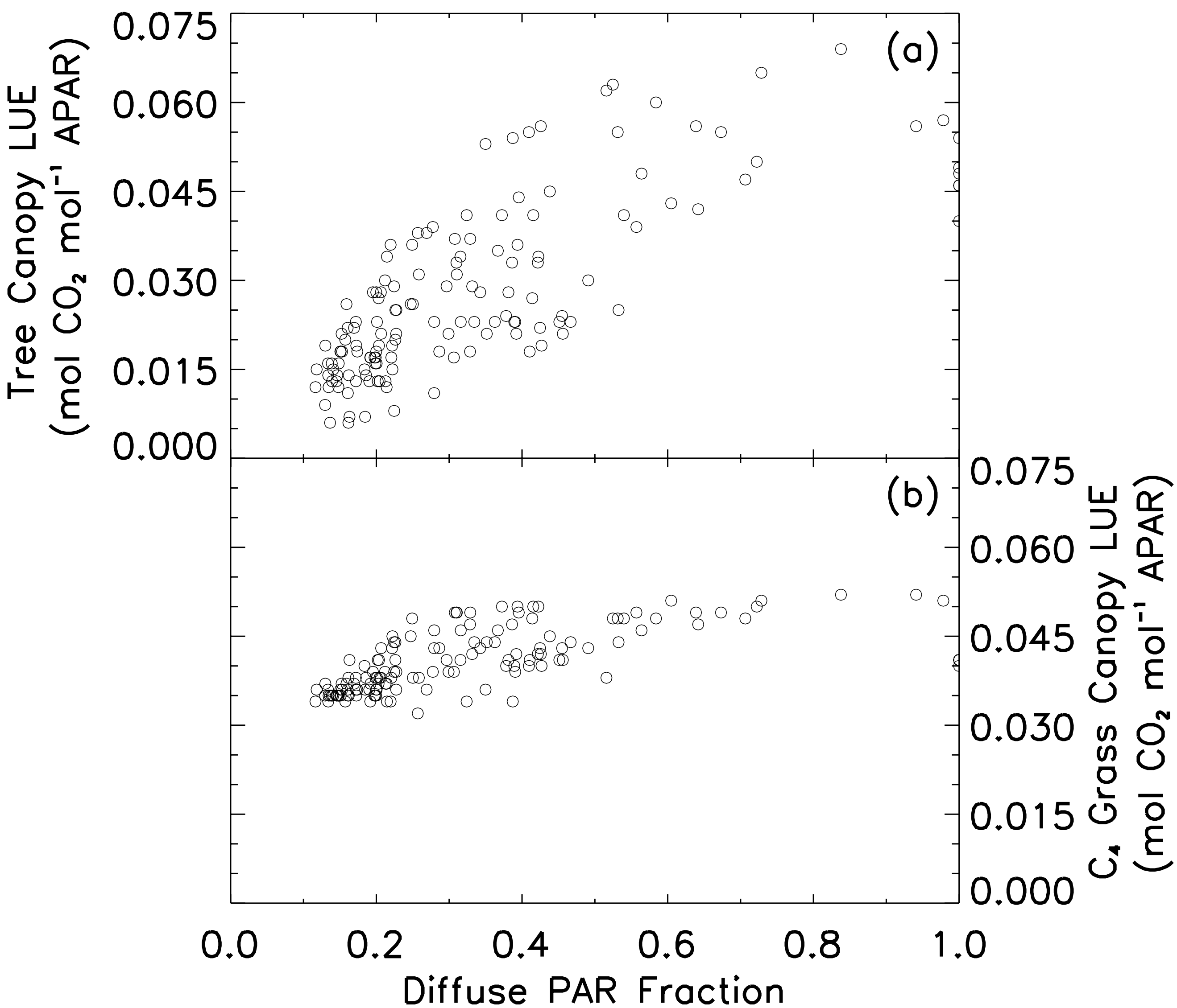

0.075
0.060
0.045
0.030
0.015
0.000
Tree Canopy LUE
(mol CO2 mol-1 APAR)
(a)
(b)
C4 Grass Canopy LUE
(mol CO2 mol-1 APAR)
0.0
0.2
0.4
0.6
0.8
1.0
Diffuse PAR Fraction

Figure 6

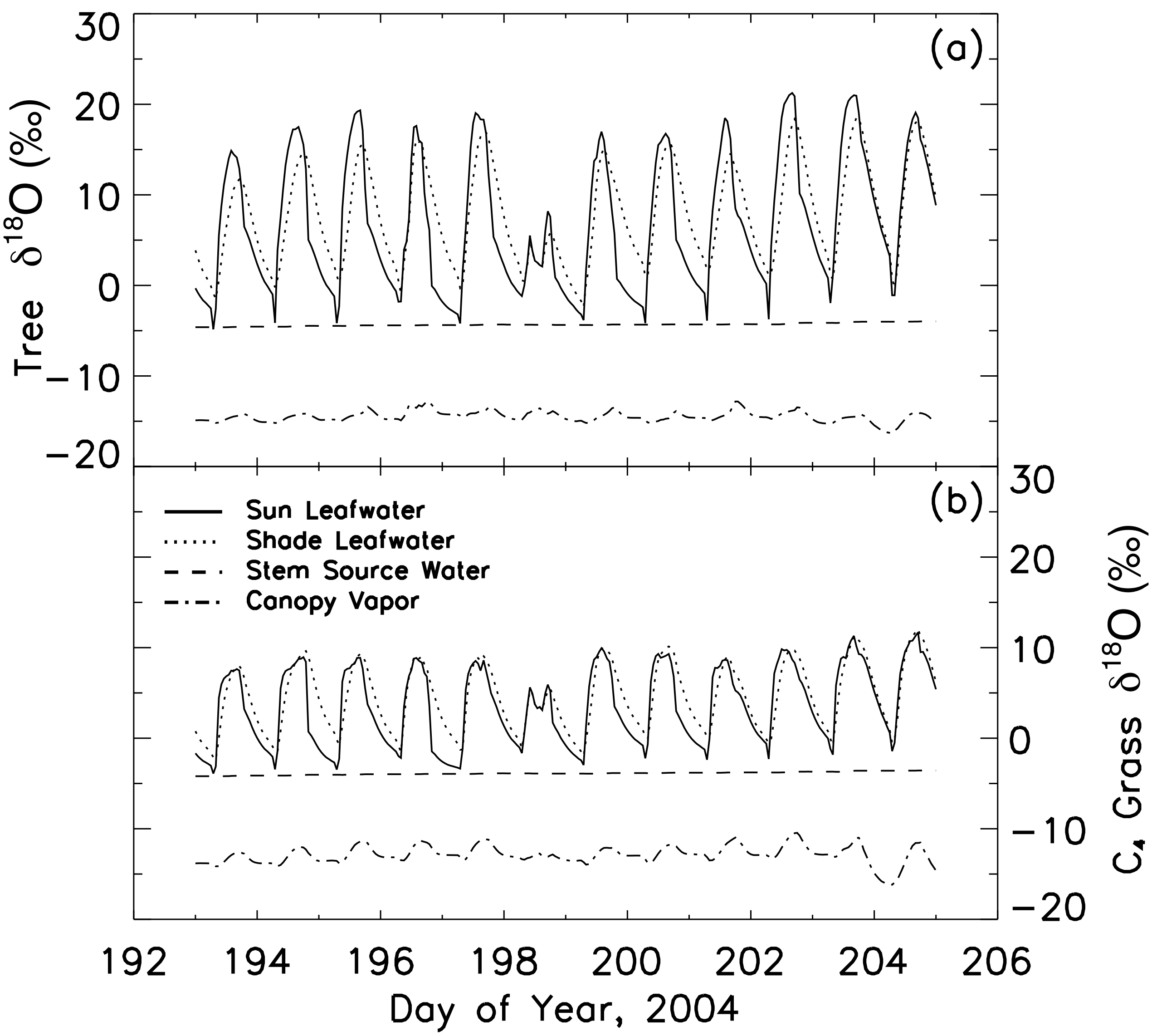

30
20
10
0
−10
−20
Tree δ18O (‰)
(a)
(b)
Sun Leafwater
Shade Leafwater
Stem Source Water
Canopy Vapor
C4 Grass δ18O (‰)
192
194
196
198
200
202
204
206
Day of Year, 2004

Figure 7

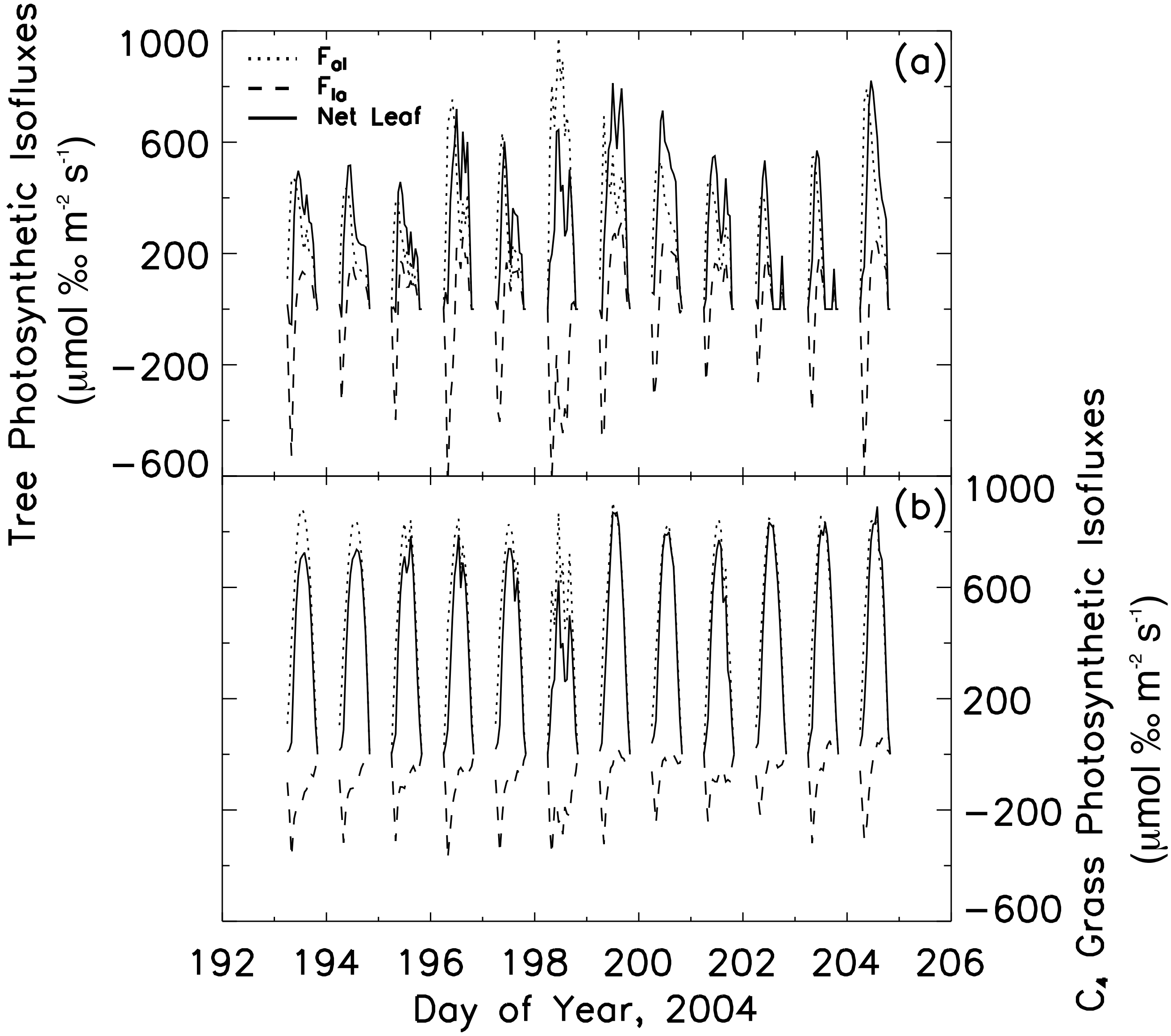

Tree Photosynthetic Isofluxes
(μmol ‰ m-2 s-1)
1000
600
200
−200
−600
Fal
Fla
Net Leaf
(a)
(b)
1000
600
200
−200
−600
C4 Grass Photosynthetic Isofluxes
(μmol ‰ m-2 s-1)
192
194
196
198
200
202
204
206
Day of Year, 2004

Figure 8

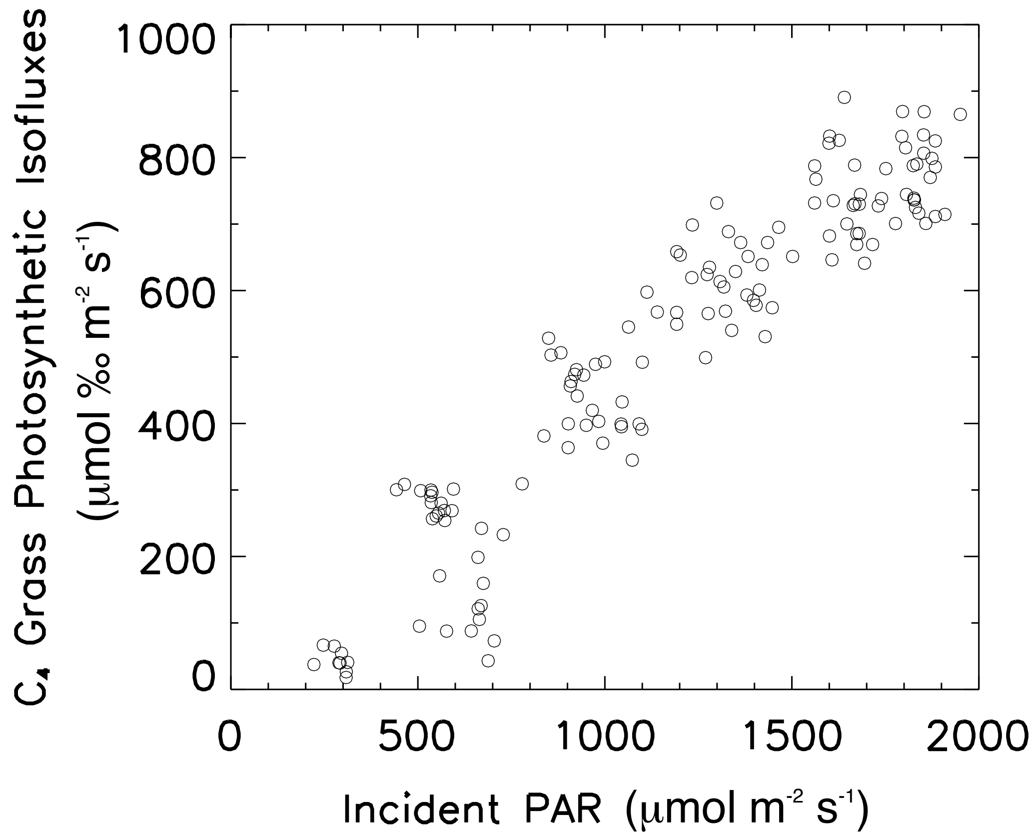
C4 Grass Photosynthetic Isofluxes
(μmol ‰ m-2 s-1)
1000
800
600
400
200
0
0
500
1000
1500
2000
Incident PAR (μmol m-2 s-1)

Figure 9

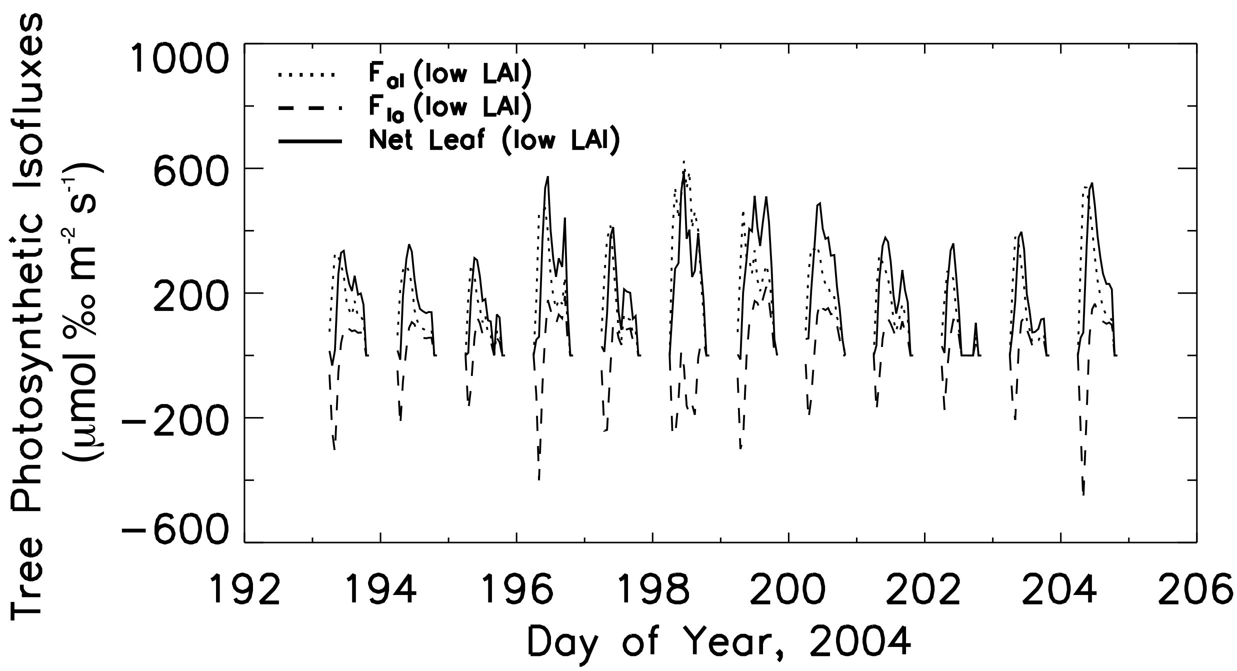
Tree Photosynthetic Isofluxes
(μmol ‰ m⁻² s⁻¹)
F_{al} (low LAI)
F_{la} (low LAI)
Net Leaf (low LAI)
1000
600
200
−200
−600
192
194
196
198
200
202
204
206
Day of Year, 2004

Figure 10